METEOROLOGICAL OFFICE
124721
2 AUG 1977
LIBRARY

MET O 11 TECHNICAL NOTE No. 91

RELATIVE PHASE SPEEDS ON STAGGERED GRIDS

DAVID A FORRESTER

RELATIVE PHASE SPEEDS ON STAGGERED GRIDS

1. INTRODUCTION

Relative phase speeds are computed for the two-dimensional shallow water equations using the time and space centred leapfrog scheme. Various grids staggered in space and time are considered and the explicit, implicit and semi-implicit cases are all treated.

2. EQUATIONS AND GRIDS

The two dimensional shallow water equations are considered in the form

$$\begin{aligned} u_t + U u_x + V u_y + g h_x &= 0 \\ v_t + U v_x + V v_y + g h_y &= 0 \\ h_t + U h_x + V h_y + \frac{c^2}{g}(u_x + v_y) &= 0 \end{aligned} \qquad (2.1)$$

Often it is sufficient to consider only the advection equations

$$\begin{aligned} u_t + U u_x + V u_y &= 0 \\ v_t + U v_x + V v_y &= 0 \\ h_t + U h_x + V h_y &= 0 \end{aligned}$$

or the gravity wave equations

$$\begin{aligned} u_t + g h_x &= 0 \\ v_t + g h_y &= 0 \\ h_t + \frac{c^2}{g}(u_x + v_y) &= 0 \end{aligned}$$

In the explicit case advection, gravity wave and shallow water equations are considered. In the implicit case only advection and gravity wave equations are considered. In the semi-implicit case (where the advection terms are treated explicitl and the gravity wave terms implicitly) only the shallow water equations are considered.

The grids considered are shown in Fig (1). Grids A, C, E, G, I, K are unstaggered in time. Grids B, D, F, H, J, L are staggered in time (and use grids A, C, E, G, I, K respectively at alternate time-steps). The grid length $\delta x \ (= \delta y)$ is the distance between two adjacent h points in the horizontal or vertical (not diagonal).

Grids A, C, E, G, I have been discussed by various authors (see Mesinger and Arakawa, 1976 and Savijärvi, 1976). Elvius and Sundström (1973) have discussed the barotropic model using grids J and D for the semi-implicit case and grids J and F for the explicit case.

Grid A (the unstaggered grid) is used by most general circulation models, including the Met O 20 11-level model.

Grid C is extensively used e.g. the semi-implicit Lax-Wendroff model, the Met O 11 semi-implicit centred model, the Met O 11 semi-implicit mesoscale model, the ECMWF centred model. Recently the UCLA GCM has been changed from grid A to grid C.

Grid D is used in the Met O 11 semi-implicit time staggered centred model.

Grid E was used in the explicit Lax-Wendroff model.

Grid G is used in the currently operational split explicit model.

Note that grids I, J, K, L are simply grids G, H, A, B respectively rotated through 45° with δx redefined.

Grids A-H admit wave numbers n, m satisfying $0 \leq n\delta x, m\delta y \leq \pi$ (This is shown in diagram D_1 of Fig (2)). Grids I-L admit wave numbers n, m satisfying $0 \leq n\delta x, m\delta y \leq 2\pi$, $n\delta x + m\delta y \leq 2\pi$ (D_2 of Fig (2)).

To see this latter point note that grid I is obtained from grid G by rotating through 45° and letting $\delta x_I = \sqrt{2}\,\delta x_G$. Thus rotating the wave space domain D_1 of Fig (2) through 45° and changing the scale by a factor of $\sqrt{2}$, one obtains the domain D_3. Now, if one assumes that U=V then there is a symmetry about the line n = m and only half the domains (shown shaded) need be considered. It is clear then that D_3 is the same as D_2. The case U≠V is considered in section 6. Changing the sign of U or V can be effected by changing the sign of n or m respectively.

The finite difference forms of the explicit equations are given for each grid in the Appendix.

3. RELATIVE PHASE SPEEDS

Assume that the variables u, v, h can be expanded as a finite fourier series, a typical term being

$$u^r_{j,k} = e^{inj\delta x}\, e^{imk\delta y}\, u^r$$

where

$$u^r = |\omega|^r\, e^{i\theta r\delta t}\, u^0$$

It is assumed that

$$u^{r+1} = \omega u^r = \omega^2 u^{r-1} \qquad (3.1)$$

where $$\omega = |\omega|\, e^{i\theta\delta t}$$

is the amplification factor.

On all 12 grids the finite difference approximations to the shallow water equations (2.1) reduce to the following equations with appropriate expressions for λ_u, λ_v, λ_{c1}, λ_{c2}.

(a) Explicit Case

$$u^{r+1} - u^{r-1} + 2i(\lambda_u + \lambda_v)u^r + 2i\lambda_{c1}h^r = 0$$

$$v^{r+1} - v^{r-1} + 2i(\lambda_u + \lambda_v)v^r + 2i\lambda_{c2}h^r = 0$$

$$h^{r+1} - h^{r-1} + 2i(\lambda_u + \lambda_v)h^r + 2i\lambda_{c1}u^r + 2i\lambda_{c2}v^r = 0$$

(b) Implicit Case

$$u^{r+1} - u^{r-1} + i(\lambda_u + \lambda_v)(u^{r+1} + u^{r-1}) + i\lambda_{c1}(h^{r+1} + h^{r-1}) = 0$$

$$v^{r+1} - v^{r-1} + i(\lambda_u + \lambda_v)(v^{r+1} + v^{r-1}) + i\lambda_{c2}(h^{r+1} + h^{r-1}) = 0$$

$$h^{r+1} - h^{r-1} + i(\lambda_u + \lambda_v)(h^{r+1} + h^{r-1}) + i\lambda_{c1}(u^{r+1} + u^{r-1}) + i\lambda_{c2}(v^{r+1} + v^{r-1}) = 0$$

(c) Semi-Implicit Case

$$u^{r+1} - u^{r-1} + 2i(\lambda_u + \lambda_v)u^r + i\lambda_{c1}(h^{r+1} + h^{r-1}) = 0$$

$$v^{r+1} - v^{r-1} + 2i(\lambda_u + \lambda_v)v^r + i\lambda_{c2}(h^{r+1} + h^{r-1}) = 0$$

$$h^{r+1} - h^{r-1} + 2i(\lambda_u + \lambda_v)h^r + i\lambda_{c1}(u^{r+1} + u^{r-1}) + i\lambda_{c2}(v^{r+1} + v^{r-1}) = 0$$

On making the assumption 3.1 these equations give rise to a quadratic:

(a) explicit case

$$\omega^2 + 2i\lambda\omega - 1 = 0$$

$$\omega = -i\lambda \pm \sqrt{1 - \lambda^2}$$

where $\lambda = \lambda_u + \lambda_v$

or $\lambda = \lambda_u + \lambda_v \pm \sqrt{\lambda_{c_1}^2 + \lambda_{c_2}^2}$

This scheme is stable if and only if $\lambda^2 \leq 1$

(b) implicit case

$$\omega^2 = \frac{1 - i\lambda}{1 + i\lambda}$$

$$\omega = \frac{\pm(1 - i\lambda)}{\sqrt{1 + \lambda^2}}$$

where λ is the same as in the explicit case.

This scheme is always stable.

(c) semi-implicit case

$$\omega^2(1 + i\lambda_c) + 2i\lambda_{uv}\omega - (1 - i\lambda_c) = 0$$

$$\omega = \frac{1}{1 + i\lambda_c}\left[-i\lambda_{uv} \pm \sqrt{1 - (\lambda_{uv}^2 - \lambda_c^2)}\right]$$

where $\lambda_{uv} = \lambda_u + \lambda_v$

and $\lambda_c = 0$

or $\lambda_c = \pm\sqrt{\lambda_{c_1}^2 + \lambda_{c_2}^2}$

This scheme is stable if and only if $\lambda_{uv}^2 - \lambda_c^2 \leq 1$

Consider now the differential equations 2.1 and expand u, v, h as infinite series, a typical term being proportional to

$$e^{inx}\, e^{imy}\, e^{i\sigma t}$$

One obtains $$-\sigma = nU + mV$$

or $$-\sigma = nU + mV \pm c\sqrt{n^2+m^2}$$

Now the relative phase speed is $$\frac{\theta}{\sigma} = \frac{\theta\,\delta t}{\sigma\,\delta t}$$

where (assuming $\delta y = \delta x$)

$$-\sigma\delta t = U\frac{\delta t}{\delta x}\, n\delta x + V\frac{\delta t}{\delta x}\, m\delta x \pm c\frac{\delta t}{\delta x}\sqrt{(n\delta x)^2 + (m\delta x)^2} \qquad (3.2)$$

and $\theta\delta t$ is obtained by solving the simultaneous equations

$$\cos(\theta\delta t) = \frac{Re(\omega)}{|\omega|}$$

$$\sin(\theta\delta t) = \frac{Im(\omega)}{|\omega|}$$

It turns out that only four expressions for $\lambda_u, \lambda_v, \lambda_{c1}, \lambda_{c2}$ need be considered. The results for all grids A-L (and possibly others) can be generated from these few cases. One is thus led to a natural classification into 4 groups referred to as 1, 2, 3, 4. The expressions for $\lambda_u, \lambda_v, \lambda_{c1}, \lambda_{c2}$ for the 4 groups are given in Table 1. Throughout this report frequent reference will be made to these groups as well as to the grids themselves.

Considering advection and gravity waves separately, one need only compute the results for the 4 groups. Table 2 then indicates which grids belong to which group.

The shallow water equations on a particular grid can be regarded as a combination of advection from one group and gravity waves from another group. Table 3 indicates the combinations for each grid. There are 16 possible combinations but only 12 grids have been considered.

Note that in the explicit case grids K and I (unstaggered in time) are in the same classifications as grids B and F (staggered in time) respectively, though the domain in wave space admitted by these grids is different.

Note also that grids D, B, J are interchanged with grids F, H, L respectively on making the transition from explicit to semi-implicit.

It has already been noted (see Table 2) that there is a great deal of degeneracy as far as advection and gravity waves are separately concerned. In fact there is even more degeneracy than is immediately apparent from Table 2.

It is easy to see that Group 3 is the same as Group 1 if $n\delta x, m\delta y$ are doubled and U, V, c are halved. Thus, for example, the explicit graphs for grid L ($0 \leq n\delta x, m\delta y \leq 2\pi$) are identical to those for grid A ($0 \leq n\delta x, m\delta y \leq \pi$). Note, however, that grid L admits only the triangular domain D_2 whereas grid A admits the square domain D_1.

Another type of degeneracy (this time accidental and not obvious from the grids) is the rotational degeneracy of the results for grids A and B. The explicit phase speed graphs for grid B are obtained from those for grid A by rotating through 45° and scaling the winds and axes by a factor of $\sqrt{2}$ viz

$$(U,V)_B = \tfrac{1}{2}(U-V, U+V)_A \qquad c_B = \frac{1}{\sqrt{2}} c_A$$

$$(n\delta x, m\delta y)_B = (n\delta x - m\delta y, n\delta x + m\delta y)_A$$

This can be seen by consideration of the expressions for $\lambda_U, \lambda_V, \lambda_{c1}, \lambda_{c2}$.

Both of the above remarks apply also to the shallow water waves.

Connected with the above remarks is the fact that grids A, B, G, H when rotated through 45° are the same as grids K, L, I, J, respectively apart from a change in scale of δx .

4. RESULTS

The relative phase speeds have been computed for

(i) advection and gravity waves separately for each of the four groups in both the explicit and implicit cases.

(ii) shallow water waves for each of the 12 grids in both the explicit and semi-implicit cases.

The graphs display contours of constant relative phase speed in the wave space (axes $n\delta x$ and $m\delta y$) of the appropriate domain for various values of the parameters $\alpha_c = c\frac{\delta t}{\delta x}$, $\alpha_U = U\frac{\delta t}{\delta x}$, $\alpha_V = V\frac{\delta t}{\delta x}$ (labelled c, U, V in the graph titles). The explicit and semi-implicit schemes are conditionally stable and some of the graphs display regions of instability indicated by +. The relative phase speed contours are plotted even in these unstable regions, the wave in the finite difference scheme being amplified. (In fact ω is pure imaginary and so the wave is a $4\delta t$ wave). Several graphs are shown for each group or grid, corresponding to different values of δt . The first graph on each page has a small value of δt and mainly represents the effect of the space truncation error. Decreasing δt further makes little significant change to the graphs. The other graphs represent the combined effects of space and time truncation as δt is increased.

Consider, firstly, the results of (i). Graphs 1, 2, 3, 4, 5, 6 display the results for the explicit scheme. Groups 2 and 3 are given on the $0-\pi$ wave domain (graphs 2, 3) and then repeated on the $0-2\pi$ domain (graphs 5, 6). Graphs 7, 8, 9, 10 display the results for the implicit scheme.

The maximum values of α_c and α_v (assuming U=V) for stability in the explicit case are given in Table 4.

Considering the explicit results on domain D_1 ($0 \leq n\delta x, m\delta y \leq \pi$), it is immediately apparent that for both advection and gravity waves Group 3 is superior to the others in phase speed accuracy, though the maximum timestep for computational stability is somewhat smaller than in the other groups.

Since none of the grids A-J discussed by Mesinger and Arakawa (1976) have the same λ's as Group 3 for both advection and gravity waves, grid L was constructed with this in mind. However, grid L admits waves on domain D_2 so is worse than expected. Moreover, grid L is identical to grid B being merely rotated through 45°. Since the finite difference schemes used here for grids L and B are equivalent, then the results must be equivalent. Thus grid L is just an alternative way of looking at grid B. The same remarks apply to grids I, J, K (equivalent to G, H, A respectively) However, especially in the case of the non-linear equations, it is possible that some finite difference schemes might be more conveniently applied to grid L than to grid B for example.

Considering now the other groups for both advection and gravity waves, Group 2 is second best, Group 1 is third and Group 4 is worst.

In the implicit case the effect of time truncation is always to worsen the phase speeds, and as δt becomes large the graphs for the different groups become very similar.

Note that time truncation becomes negligible in the limit of small α's i.e. small δt or slow waves. Thus time truncation is almost certainly negligible in any realistic model for all but the fastest gravity and advection waves.
As can be seen from the graphs, the errors due to explicit time truncation (in this case the leapfrog scheme) tend to cancel out the errors due to space truncation. Use of the largest possible δt for each wave would give better results.

In a semi-implicit model the fast gravity waves (which are treated implicitly) are inaccurately represented and, of the explicitly treated gravity waves, those most accurately represented are the fastest ones. In an explicit model all gravity waves except the fastest are inaccurately represented.

Now consider the results of (ii). Graphs were obtained for all 12 grids for various values of α_c, α_u, α_v. For simplicity it was decided to choose $\alpha_u = \alpha_v$ (but see section 6 for the case $\alpha_u \neq \alpha_v$) and consider only the three values $\alpha_u/\alpha_c = 1, 2, 1/3$.

Only the explicit graphs for $\alpha_u/\alpha_c = 1$ are included in this report (graphs 11 - 22); the other two values give very similar results, the exact form of the shallow water wave graphs depending on whether advection or gravity waves dominate.

The graphs corresponding to small δt (space truncation only) apply also to the semi-implicit case provided the time staggered grids D, B, J are interchanged with F, H, L respectively.

Among the grids A-H it is clear that

(a) B is better than A

(b) D is better than C

(c) F is better than E

(d) G is similar to H

(e) F is best overall

(f) B is a close second best

(g) In order of decreasing accuracy, the remaining grids come roughly

C, G = H, D, E, A

Turning now to grids I-L

(h) I is similar to J

(i) L is better than K

Because of the relationship between grids I, J, K, L and G, H, A, B respectively comment (h) is the same as (d) and comment (i) is the same as (a).

Note that the ordering of the grids given in (g) above may be slightly variable depending on the ratio U/c. One finds that the graphs for grids A, B, E, K, L are almost independent of U/c, for grids C, F, G, I are slightly better when gravity waves dominate (e.g. $U/c = 1/3$) and for grids D, H, J are slightly better when advection dominates (eg $U/c = 2$). This can be inferred from Table 2 and the results of (i).

In conclusion, of the 12 grids considered in this report, the grid to give the best phase speed accuracy for an explicit model is grid F and for a semi-implicit model is grid D. However, grid B gives almost as good results for the explicit scheme and grid H for the semi-implicit scheme. Grids L, K are useful alternatives to grids B, A respectively.

5. MAXIMUM TIMESTEP FOR COMPUTATIONAL STABILITY

The condition $|\omega| \leq 1$ for computational stability is now investigated to obtain the maximum timestep δt permitted over the whole domain of wave numbers n, m for given c, U, V. To obtain the result it is necessary to vary the direction of the advection wind keeping $\sqrt{U^2+V^2}$ constant. The results are given in Table 5 for the explicit case and Table 6 for the semi-implicit case.

The maximum value of the quantity $\sqrt{U^2+V^2}\,\frac{\delta t}{\delta x}$ (varying n, m over the appropriate domain) is given for various values of $c/\sqrt{U^2+V^2}$ for the 12 grids. In the case $\sqrt{U^2+V^2} = 0$ (denoted $c/\sqrt{U^2+V^2} = \infty$) the maximum value of $c\,\frac{\delta t}{\delta x}$ is given.

Firstly, in the explicit case, the condition is $\lambda^2 \leq 1$

where $$\lambda = \lambda_U + \lambda_V + \lambda_c$$

Writing $\lambda_u = \alpha_u Q_u \qquad \lambda_v = \alpha_v Q_v \qquad \lambda_c = \alpha_c Q_c$

where $\alpha_u = u \frac{\delta t}{\delta x} \qquad \alpha_v = v \frac{\delta t}{\delta x} \qquad \alpha_c = c \frac{\delta t}{\delta x}$

the condition becomes

$$| \alpha_u Q_u + \alpha_v Q_v + \alpha_c Q_c | \leq 1$$

Now allowing the direction of the advection wind to vary, keeping $\sqrt{u^2+v^2}$ constant, one finds that the condition reduces to

$$| \alpha \sqrt{Q_u^2 + Q_v^2} + \alpha_c Q_c | \leq 1$$

where

$$\alpha = \sqrt{u^2+v^2} \frac{\delta t}{\delta x}$$

Secondly, in the semi-implicit case, the condition is

$$\lambda_{uv}^2 - \lambda_c^2 \leq 1$$

Introducing the same notation as before, and varying the direction of the advection wind one finds

$$\alpha^2 (Q_u^2 + Q_v^2) - \alpha_c^2 Q_c^2 \leq 1$$

Note that if the left hand side of this inequality is zero or negative for all n, m then the scheme is unconditionally stable (for these particular values of c and $\sqrt{u^2+v^2}$).

Notice from Table 6 that if $c/\sqrt{u^2+v^2} \geq 1.0$ the semi-implicit scheme is unconditionally stable on grids A, C, D, G, H, I, J, K but is still only conditionally stable on grids B, E, F, L if $\sqrt{u^2+v^2} \neq 0$ however large c may be.

It is however only certain wave numbers which may become unstable - all other wave numbers are stable for $c/\sqrt{u^2+v^2} \geq 1.0$. For example, for $c/\sqrt{u^2+v^2} = 10.0$ the unstable wave numbers are:-

grids B and F	$(n\delta x, m\delta y)$	$= (\pi, 0)$ or $(0, \pi)$
grid E		$= (\pi, \pi/2)$ or $(\pi/2, \pi)$
grid L		$= (\pi, \pi)$

Notice also that for fixed $\sqrt{u^2+v^2}$, as c increases δt_{MAX} decreases in the explicit case, but increases (or remains constant) in the semi-implicit case. Thus in a multi-level model in which some waves are treated explicitly and others implicitly, the maximum time-step is always determined by the speed of the fastest explicit wave. If all the waves are treated implicitly, then the time-step is determined by the speed of the slowest wave.

For an explicit model with $c = 300\ ms^{-1}$ or $c = 100\ ms^{-1}$ and $\sqrt{u^2+v^2} = 50\ ms^{-1}$ to $100\ ms^{-1}$ the largest time-step is permitted on grids D and E (grids A and H are next). For an explicit model with $c = 50\ ms^{-1}$ and the same $\sqrt{u^2+v^2}$, grids D and E still permit the largest time-step, but grids A, C, G, H allow almost as large time-steps.

For a semi-implicit model with $c = 300\ ms^{-1}$ or $c = 100\ ms^{-1}$ and $\sqrt{u^2+v^2} = 50\ ms^{-1}$ to $100\ ms^{-1}$ grids A, C, D, G, H are unconditionally stable, but grids B, E, F have a maximum time-step. With $c = 50\ ms^{-1}$ and $\sqrt{u^2+v^2} = 100\ ms^{-1}$ all grids have a maximum timestep.

6. THE CASE U≠V

In section 4 it was, for convenience, always assumed that U=V. Since this is obviously hardly ever true in an actual model, it is important to consider the effect on the phase speeds of varying the direction of the wind. An analysis similar to that given in section 5 for investigating the maximum time-step for stability seems not to be possible when analysing the phase speeds or relative phase speeds for the following reason.

From equation 3.2 (taking $\epsilon = 0$ here) it is clear that $\sigma\delta t$ may vanish when U and V have opposite signs. It is also clear that $\theta\delta t$ will vanish along some curve when U and V have opposite signs. However, this curve $\theta\delta t = 0$ does not coincide with the curve $\sigma\delta t = 0$ except in the special case U = -V. Thus, in general, the relative phase speed θ/σ will have a singularity along the line $\sigma\delta t = 0$.

It is more instructive therefore to plot the phases $\theta\delta t$ and $\sigma\delta t$ in wave space rather than the relative phase θ/σ.

The 4 groups have been examined for advection with $U \neq V$ for small δt on the wave domain D_1 $(0 \leq n\delta x, m\delta y \leq \pi)$ The quantity $\sqrt{U^2+V^2}\,\frac{\delta t}{\delta x}$ was kept constant $(= 0.01 \times \sqrt{2})$ and V/U was varied from +1 to -1.

As V/U is varied, the phase of the longer waves changes rather slowly compared with the phase of the shorter waves, and the longer waves maintain roughly the same relative accuracy whereas the shorter waves may not e.g. in group 1 with U=-V the relative phase is -1.0 for $(2\delta x, 2\delta y)$ waves.

In fact the behaviour is slightly different for the different groups 1, 2, 3, 4. For groups 1 and 3 the phase speeds with V/U = -1 are worse than those with V/U = +1. For group 2, V/U = -1 is better than V/U = +1. For group 4, V/U = -1 is slightly worse than V/U = +1.

The curves $\sigma\delta t = 0$ and $\theta\delta t = 0$ and the region between them present no problem.

REFERENCES

ELVIUS, T and SUNDSTRÖM, A. 1973 Tellus 25, 132

MESINGER, F and ARAKAWA, A. 1976 "Numerical Methods used in Atmospheric Models" Vol 1. GARP Publications Series No. 17.

SAVIJÄRVI, H. 1976 "Computational Dispersion of Gravity-Inertia Waves in Various Difference Schemes" Report No. 10, Dept of Meteorology, Helsinki University.

APPENDIX

EXPLICIT FINITE DIFFERENCE EQUATIONS FOR THE GRIDS A - L

(A)

$$u_{2t} + U u_{2x} + V u_{2y} + g h_{2x} = 0$$

$$v_{2t} + U v_{2x} + V v_{2y} + g h_{2y} = 0$$

$$h_{2t} + U h_{2x} + V h_{2y} + \frac{c^2}{g}(u_{2x} + v_{2y}) = 0$$

(B)

$$u_{2t} + U \bar{u}^{y}_{x} + V \bar{u}^{x}_{y} + g \bar{h}^{y}_{x} = 0$$

$$v_{2t} + U \bar{v}^{y}_{x} + V \bar{v}^{x}_{y} + g \bar{h}^{x}_{y} = 0$$

$$h_{2t} + U \bar{h}^{y}_{x} + V \bar{h}^{x}_{y} + \frac{c^2}{g}(\bar{u}^{y}_{x} + \bar{u}^{x}_{y}) = 0$$

(C)

$$u_{2t} + U u_{2x} + V u_{2y} + g h_{x} = 0$$

$$v_{2t} + U v_{2x} + V v_{2y} + g h_{y} = 0$$

$$h_{2t} + U h_{2x} + V h_{2y} + \frac{c^2}{g}(u_{x} + v_{y}) = 0$$

(D)

$$u_{2t} + U \bar{u}^{y}_{x} + V \bar{u}^{x}_{y} + g \bar{h}^{y}_{2x} = 0$$

$$v_{2t} + U \bar{v}^{y}_{x} + V \bar{v}^{x}_{y} + g \bar{h}^{x}_{2y} = 0$$

$$h_{2t} + U \bar{h}^{y}_{x} + V \bar{h}^{x}_{y} + \frac{c^2}{g}(\bar{u}^{y}_{2x} + \bar{v}^{x}_{2y}) = 0$$

(E)

$$u_{2t} + U u_{2x} + V u_{2y} + g \bar{h}^{y}_{2x} = 0$$

$$v_{2t} + U v_{2x} + V v_{2y} + g \bar{h}^{x}_{2y} = 0$$

$$h_{2t} + U h_{2x} + V h_{2y} + \frac{c^2}{g}(\bar{u}^{y}_{2x} + \bar{v}^{x}_{2y}) = 0$$

(F)

$$u_{2t} + U \bar{u}^{y}_{x} + V \bar{u}^{x}_{y} + g h_{x} = 0$$

$$v_{2t} + U \bar{v}^{y}_{x} + V \bar{v}^{x}_{y} + g h_{y} = 0$$

$$h_{2t} + U \bar{h}^{y}_{x} + V \bar{h}^{x}_{y} + \frac{c^2}{g}(u_{x} + v_{y}) = 0$$

(G)
$$u_{2t} + U u_{2x} + V u_{2y} + g \bar{h}^{y}_{x} = 0$$
$$v_{2t} + U v_{2x} + V v_{2y} + g \bar{h}^{x}_{y} = 0$$
$$h_{2t} + U h_{2x} + V h_{2y} + \frac{c^2}{g}\left(\bar{u}^{y}_{x} + \bar{v}^{x}_{y}\right) = 0$$

(H)
$$u_{2t} + U \bar{u}^{y}_{x} + V \bar{u}^{x}_{y} + g h_{2x} = 0$$
$$v_{2t} + U \bar{v}^{y}_{x} + V \bar{v}^{x}_{y} + g h_{2y} = 0$$
$$h_{2t} + U \bar{h}^{y}_{x} + V \bar{h}^{x}_{y} + \frac{c^2}{g}\left(u_{2x} + v_{2y}\right) = 0$$

(I)
$$u_{2t} + U \bar{u}^{y}_{x} + V \bar{u}^{x}_{y} + g h_{x} = 0$$
$$v_{2t} + U \bar{v}^{y}_{x} + V \bar{v}^{x}_{y} + g h_{y} = 0$$
$$h_{2t} + U \bar{h}^{y}_{x} + V \bar{h}^{x}_{y} + \frac{c^2}{g}\left(u_{x} + v_{y}\right) = 0$$

(same as F)

(J)
$$u_{2t} + U u_{x} + V u_{y} + g \bar{h}^{y}_{x} = 0$$
$$v_{2t} + U v_{x} + V v_{y} + g \bar{h}^{x}_{y} = 0$$
$$h_{2t} + U h_{x} + V h_{y} + \frac{c^2}{g}\left(\bar{u}^{y}_{x} + \bar{v}^{x}_{y}\right) = 0$$

(K)
$$u_{2t} + U \bar{u}^{y}_{x} + V \bar{u}^{x}_{y} + g \bar{h}^{y}_{x} = 0$$
$$v_{2t} + U \bar{v}^{y}_{x} + V \bar{v}^{x}_{y} + g \bar{h}^{x}_{y} = 0$$
$$h_{2t} + U \bar{h}^{y}_{x} + V \bar{h}^{x}_{y} + \frac{c^2}{g}\left(\bar{u}^{y}_{x} + \bar{v}^{x}_{y}\right) = 0$$

(same as B)

(L)
$$u_{2t} + U u_{x} + V u_{y} + g h_{x} = 0$$
$$v_{2t} + U v_{x} + V v_{y} + g h_{y} = 0$$
$$h_{2t} + U h_{x} + V h_{y} + \frac{c^2}{g}\left(u_{x} + v_{y}\right) = 0$$

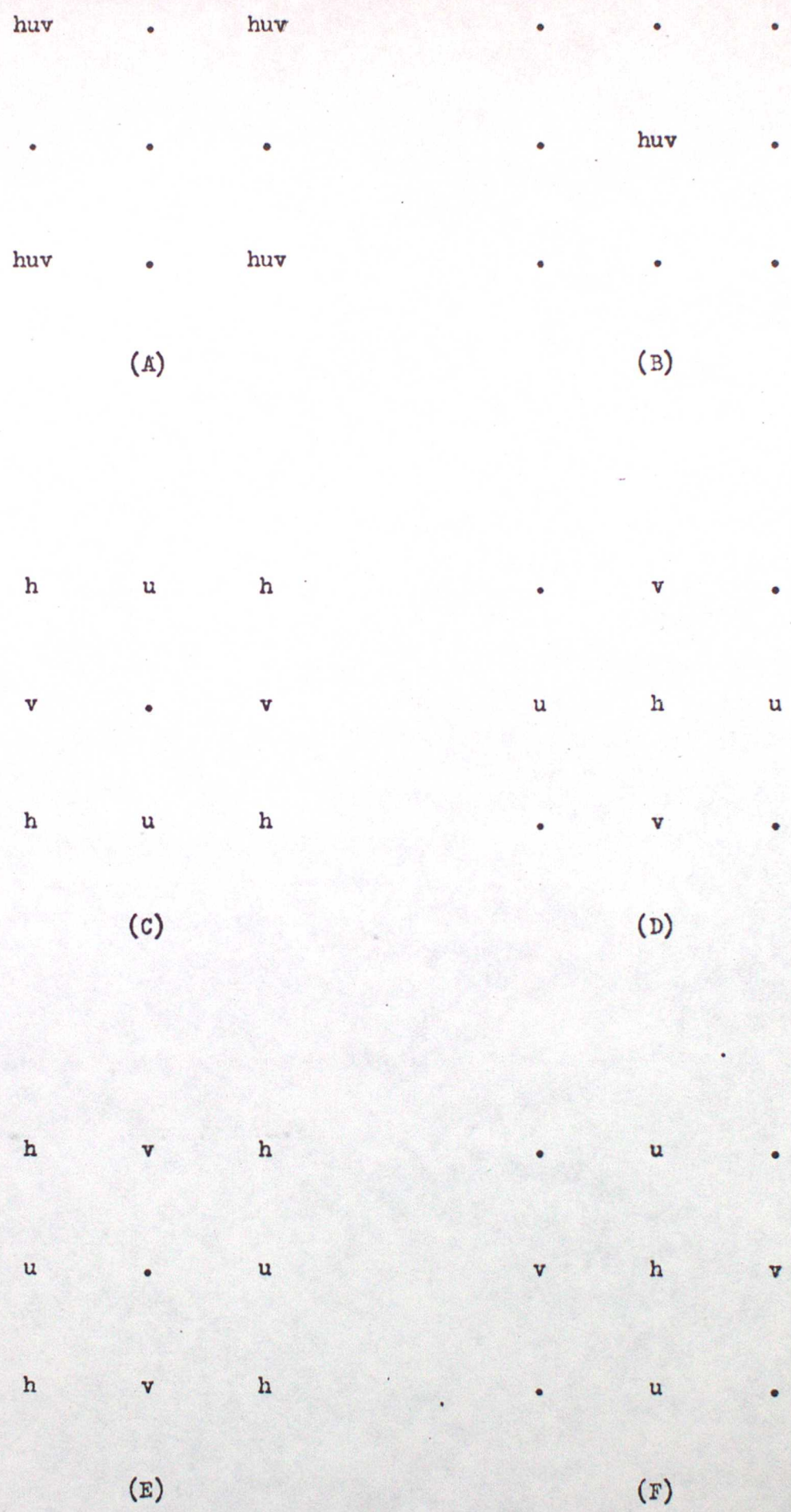

Fig. (1)

h . h

. uv .

h . h

(G)

uv . uv

. h .

uv . uv

(H)

h uv h

uv h uv

h uv h

(I)

uv h uv

h uv h

uv h uv

(J)

huv . huv

. huv .

huv . huv

(K)

. huv .

huv . huv

. huv .

(L)

Fig. (1) cont.

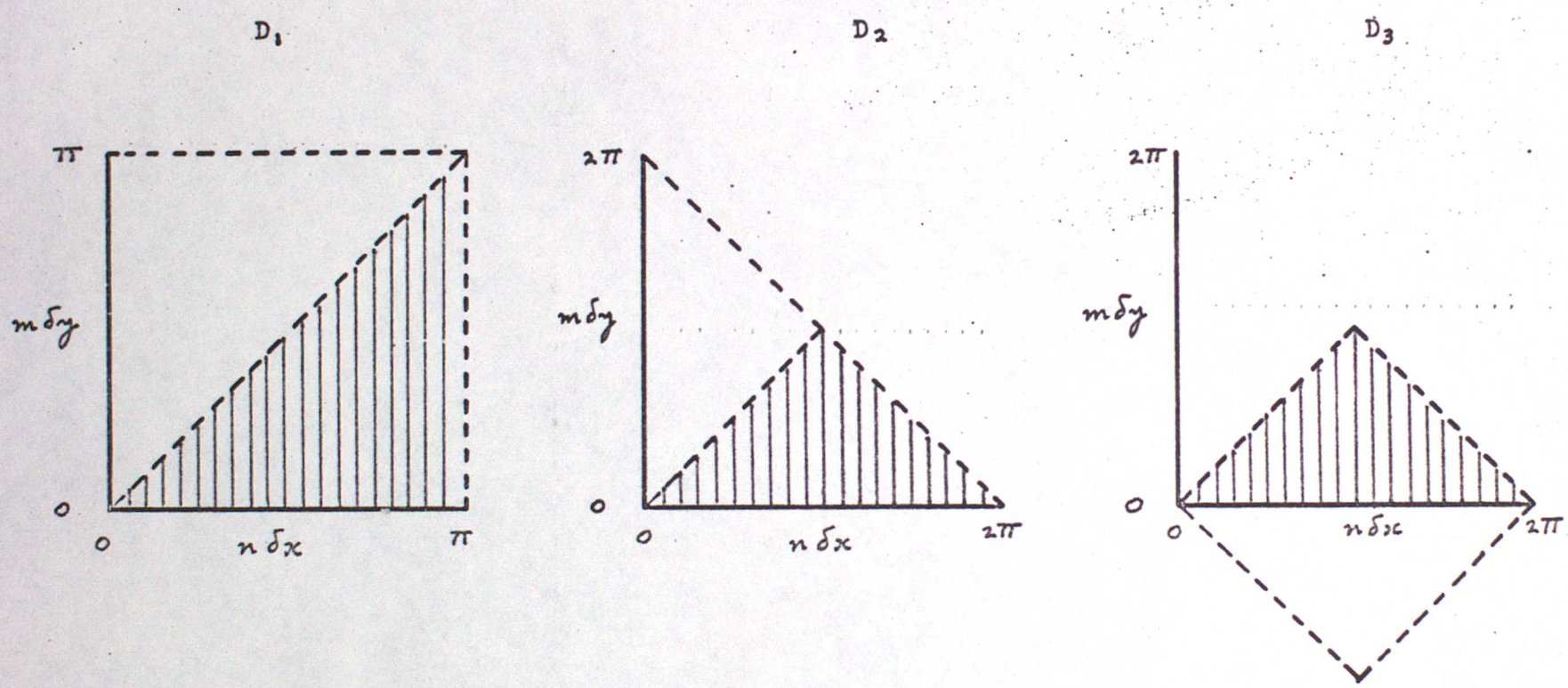

Fig.(2)

Domains in wave space. Grids A - H admit D_1, grids I - L admit D_2.
Only the shaded regions need be considered in the symmetric case U=V.

	ADVECTION	GRAVITY WAVES
GROUP 1	$\lambda_u = U\frac{\delta t}{\delta x}\sin n\delta x$	$\lambda_{c1} = c\frac{\delta t}{\delta x}\sin n\delta x$
	$\lambda_v = V\frac{\delta t}{\delta y}\sin m\delta y$	$\lambda_{c2} = c\frac{\delta t}{\delta y}\sin m\delta y$
GROUP 2	$\lambda_u = U\frac{\delta t}{\delta x}\,2\sin\frac{1}{2}n\delta x\cos\frac{1}{2}m\delta y$	$\lambda_{c1} = c\frac{\delta t}{\delta x}\,2\sin\frac{1}{2}n\delta x\cos\frac{1}{2}m\delta y$
	$\lambda_v = V\frac{\delta t}{\delta y}\,2\sin\frac{1}{2}m\delta y\cos\frac{1}{2}n\delta x$	$\lambda_{c2} = c\frac{\delta t}{\delta y}\,2\sin\frac{1}{2}m\delta y\cos\frac{1}{2}n\delta x$
GROUP 3	$\lambda_u = U\frac{\delta t}{\delta x}\,2\sin\frac{1}{2}n\delta x$	$\lambda_{c1} = c\frac{\delta t}{\delta x}\,2\sin\frac{1}{2}n\delta x$
	$\lambda_v = V\frac{\delta t}{\delta y}\,2\sin\frac{1}{2}m\delta y$	$\lambda_{c2} = c\frac{\delta t}{\delta y}\,2\sin\frac{1}{2}m\delta y$
GROUP 4	$\lambda_u = U\frac{\delta t}{\delta x}\sin n\delta x\cos\frac{1}{2}m\delta y$	$\lambda_{c1} = c\frac{\delta t}{\delta x}\sin n\delta x\cos\frac{1}{2}m\delta y$
	$\lambda_v = V\frac{\delta t}{\delta y}\sin m\delta y\cos\frac{1}{2}n\delta x$	$\lambda_{c2} = c\frac{\delta t}{\delta y}\sin m\delta y\cos\frac{1}{2}n\delta x$

Table 1. λ's for the 4 Groups

	ADVECTION		GRAVITY WAVES	
	$0 \leq \begin{matrix} n\delta x \\ m\delta y \end{matrix} \leq \pi$	$0 \leq \begin{matrix} n\delta x \\ m\delta y \end{matrix} \leq 2\pi$	$0 \leq \begin{matrix} n\delta x \\ m\delta y \end{matrix} \leq \pi$	$0 \leq \begin{matrix} n\delta x \\ m\delta y \end{matrix} \leq 2\pi$
GROUP 1	A C E G		A H	
GROUP 2	B D F H	I K	B G	J K
GROUP 3		J L	C F	I L
GROUP 4			D E	

Table 2.

Classification of the 12 grids into 4 groups for the explicit advection and gravity waves.

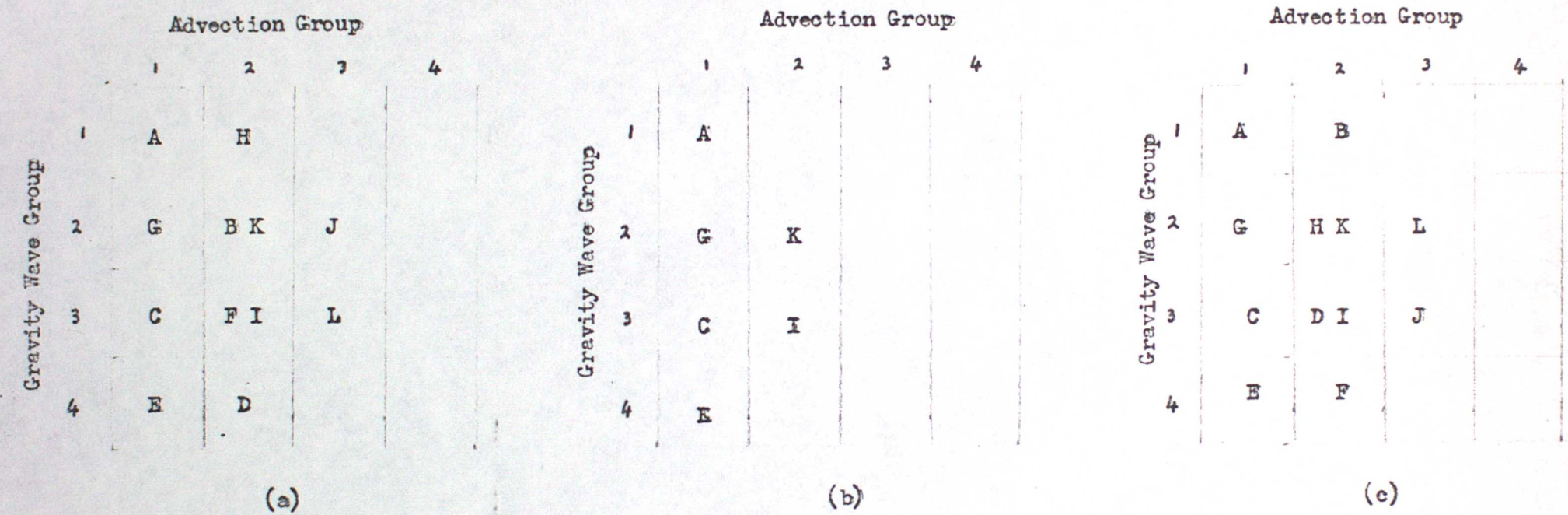

Table 3.

Classification of the grids for the shallow water equations in the (a) explicit, (b) implicit, (c) semi-implicit cases.

	MAXIMUM $c\frac{\delta t}{\delta x}$ for gravity waves	MAXIMUM $U\frac{\delta t}{\delta x}$ for advection with U=V
Group 1	0.7071	0.5
Group 2	0.5	0.5
Group 3	0.3536	0.25
Group 4	0.91	0.65

TABLE 4

Maximum α_c and α_U (assuming U=V) for computational stability of gravity waves and advection.

$c/\sqrt{U^2+V^2}$	A	B	C	D	E	F	G	H	I	J	K	L
0.0	0.71	0.50	0.71	0.50	0.71	0.50	0.71	0.50	0.50	0.35	0.50	0.35
0.1	0.64	0.45	0.62	0.49	0.66	0.45	0.64	0.49	0.45	0.35	0.45	0.32
0.5	0.47	0.33	0.40	0.45	0.52	0.33	0.47	0.45	0.33	0.32	0.33	0.24
1.0	0.35	0.25	0.27	0.38	0.41	0.25	0.35	0.35	0.25	0.25	0.25	0.18
2.0	0.23	0.17	0.16	0.28	0.28	0.16	0.22	0.23	0.16	0.17	0.17	0.12
3.0	0.18	0.13	0.11	0.22	0.22	0.11	0.16	0.18	0.11	0.125	0.125	0.088
4.0	0.14	0.10	0.086	0.17	0.17	0.085	0.12	0.14	0.086	0.10	0.10	0.071
5.0	0.12	0.083	0.069	0.15	0.15	0.069	0.098	0.12	0.069	0.083	0.083	0.059
10.0	0.064	0.045	0.035	0.082	0.082	0.035	0.050	0.064	0.035	0.045	0.045	0.032
∞	0.71	0.50	0.35	0.92	0.92	0.35	0.50	0.71	0.35	0.50	0.50	0.35

Table 5 (EXPLICIT CASE)

The maximum value of $\sqrt{U^2+V^2}\,\frac{\delta t}{\delta x}$ for given $c/\sqrt{U^2+V^2}$ for the 12 grids.
In the case $\sqrt{U^2+V^2}=0$ (denoted $c/\sqrt{U^2+V^2}=\infty$) the maximum value of $c\,\frac{\delta t}{\delta x}$ is given.

$c/\sqrt{u^2+v^2}$	A	B	C	D	E	F	G	H	I	J	K	L
0.0	0.71	0.50	0.71	0.50	0.71	0.50	0.71	0.50	0.50	0.35	0.50	0.35
0.1	0.71	0.50	0.71	0.50	0.71	0.50	0.71	0.50	0.50	0.35	0.50	0.35
0.5	0.82	0.50	0.94	0.57	0.76	0.50	0.82	0.57	0.58	0.41	0.58	0.35
1.0	-	0.50	-	-	0.92	0.50	-	-	-	-	-	0.35
2.0	-	0.50	-	-	1.00	0.50	-	-	-	-	-	0.35
3.0	-	0.50	-	-	1.00	0.50	-	-	-	-	-	0.35
4.0	-	0.50	-	-	1.00	0.50	-	-	-	-	-	0.35
5.0	-	0.50	-	-	1.00	0.50	-	-	-	-	-	0.35
10.0	-	0.50	-	-	1.00	0.50	-	-	-	-	-	0.35
∞	-	-	-	-	-	-	-	-	-	-	-	-

Table 6 (SEMI-IMPLICIT CASE)

The maximum value of $\sqrt{u^2+v^2}\,\frac{\delta t}{\delta x}$ for given $c/\sqrt{u^2+v^2}$ for the 12 grids.

In the case $\sqrt{u^2+v^2} = 0$ (denotated $c/\sqrt{u^2+v^2} = \infty$) the maximum value of $c\frac{\delta t}{\delta x}$ is given.

(- indicates that the scheme is stable for all $\sqrt{u^2+v^2}\,\frac{\delta t}{\delta x}$, or $c\frac{\delta t}{\delta x}$ in the case $\sqrt{u^2+v^2} = 0$).

NOTES ON GRAPHS

The following graphs display contours of constant relative phase speed in wave space, the axes being $n\delta x$ and $m\delta y$, for various values of the dimensionless parameters $c\frac{\delta t}{\delta x}$, $U\frac{\delta t}{\delta x}$, $V\frac{\delta t}{\delta x}$ (labelled c, U, V in the graph titles). In some of the graphs regions of instability appear indicated by +.

Since only the case U=V is considered, all the graphs are symmetrical about $n\delta x = m\delta y$.

Graphs 5, 6 and 19-22 which refer to grids I-L cover wave numbers in the range $0 - 2\pi$. However, only the triangular region $n\delta x + m\delta y \leq 2\pi$ is relevant. All other graphs cover wave numbers in the range $0 - \pi$.

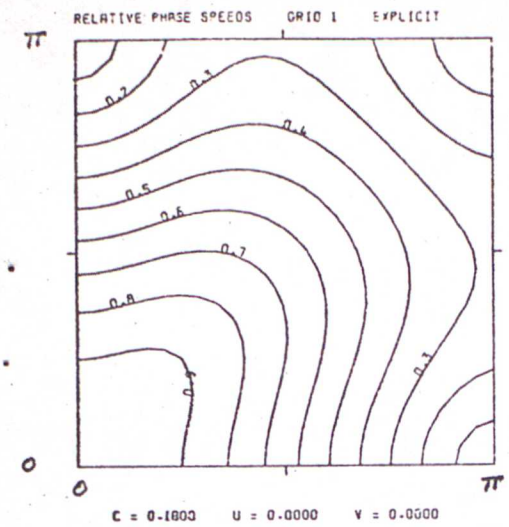

C = 0.1803 U = 0.0000 V = 0.0000

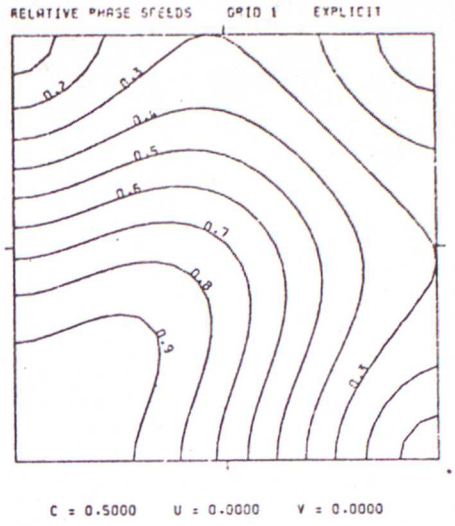

C = 0.5000 U = 0.0000 V = 0.0000

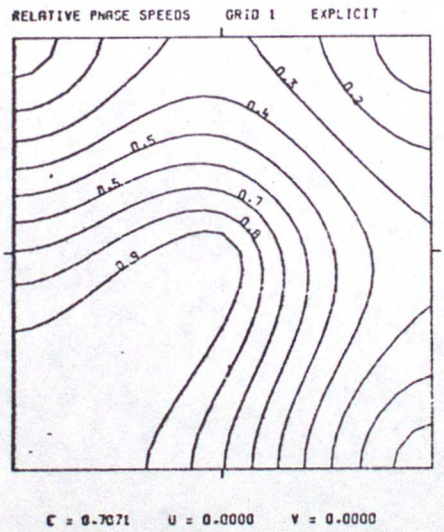

C = 0.7071 U = 0.0000 V = 0.0000

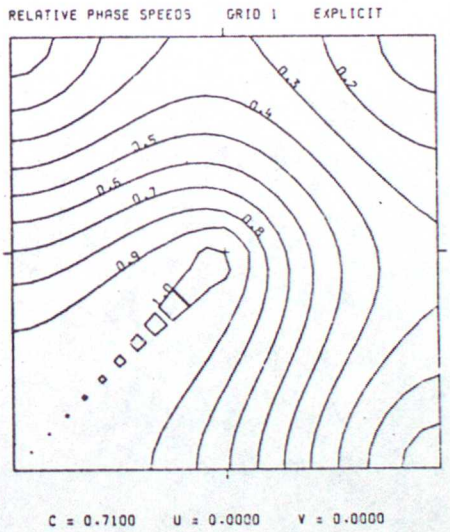

C = 0.7100 U = 0.0000 V = 0.0000

Graph 1(a) GROUP 1 EXPLICIT GRAVITY WAVES

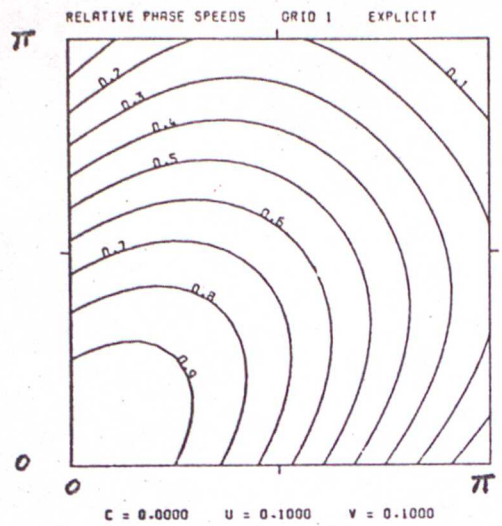

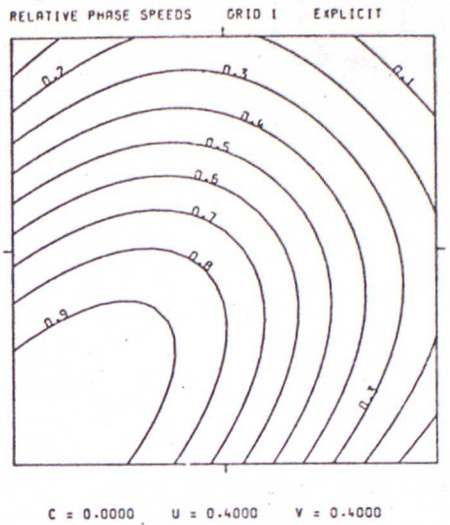

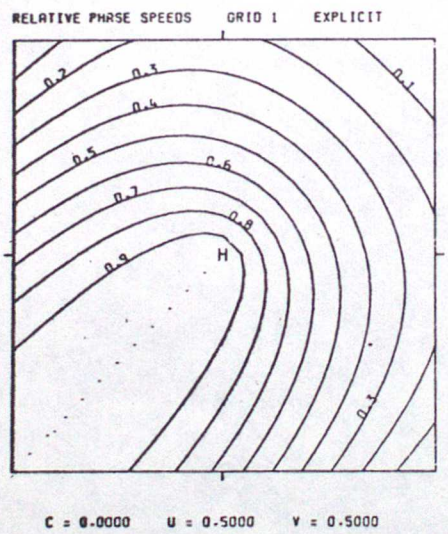

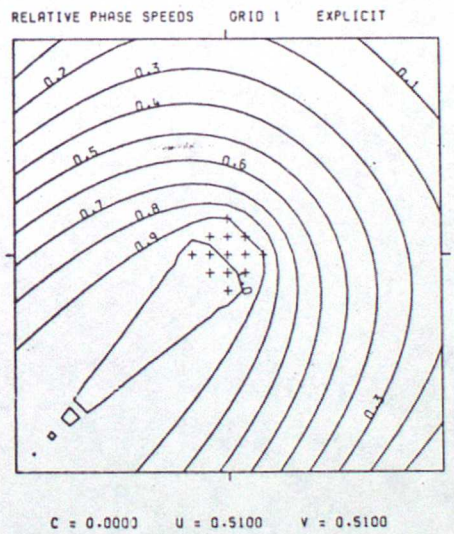

Graph 1(b) GROUP 1 EXPLICIT ADVECTION

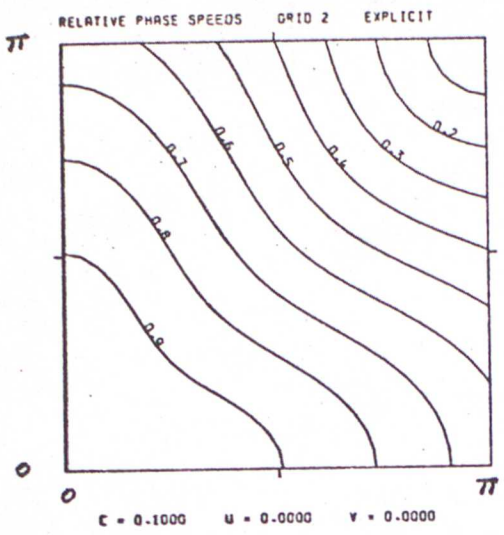

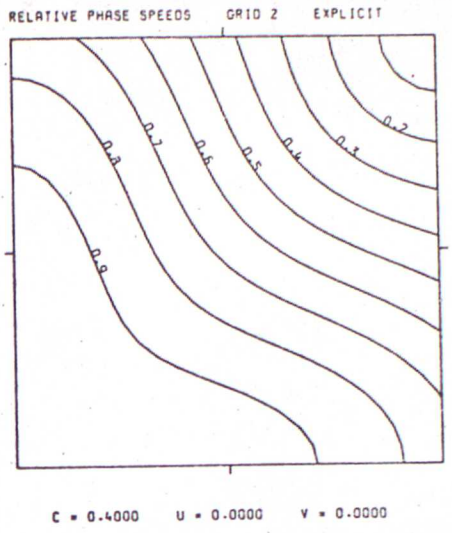

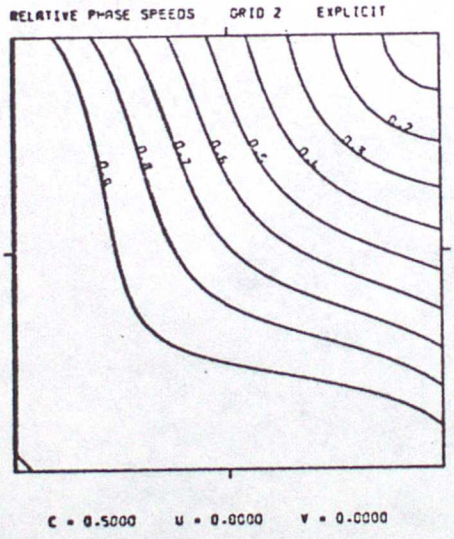

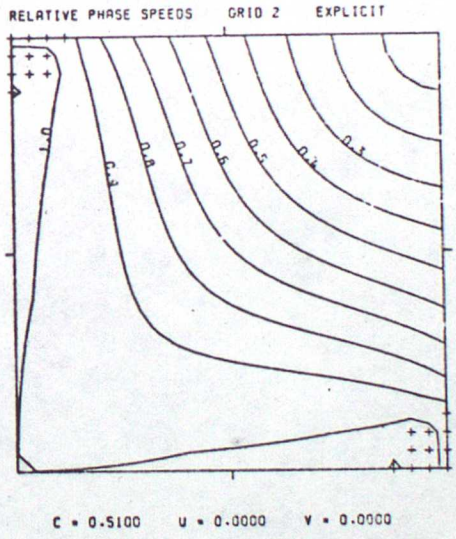

Graph 2(a) GROUP 2 EXPLICIT GRAVITY WAVES

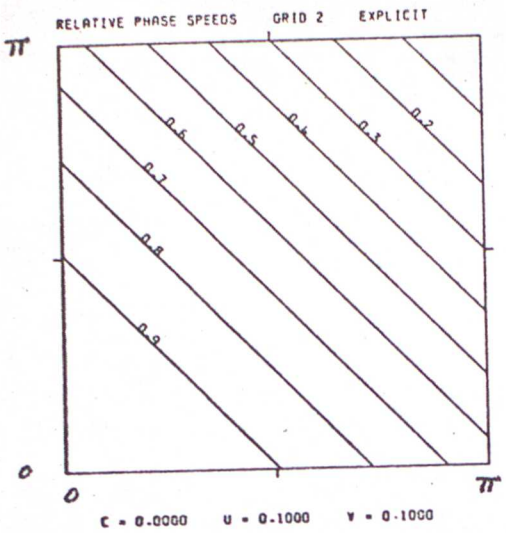

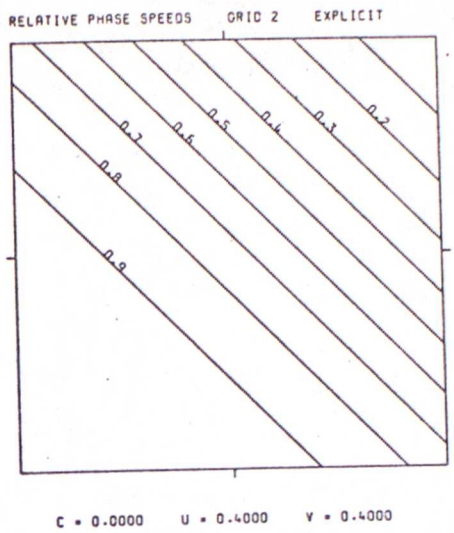

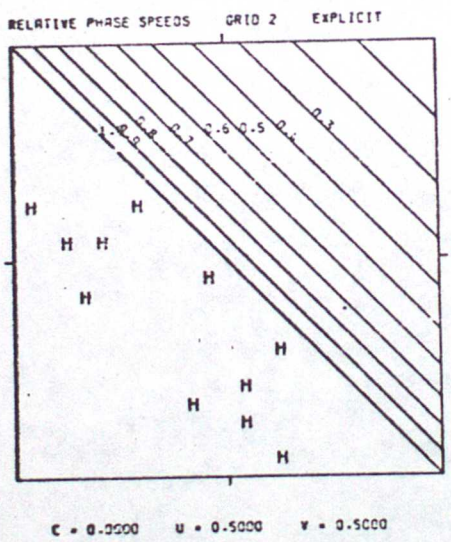

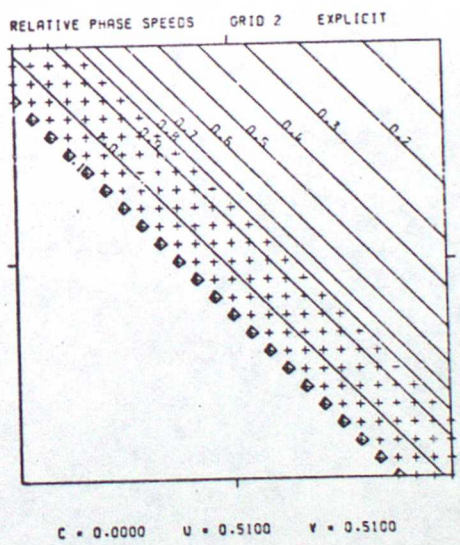

Graph 2(b) GROUP 2 EXPLICIT ADVECTION

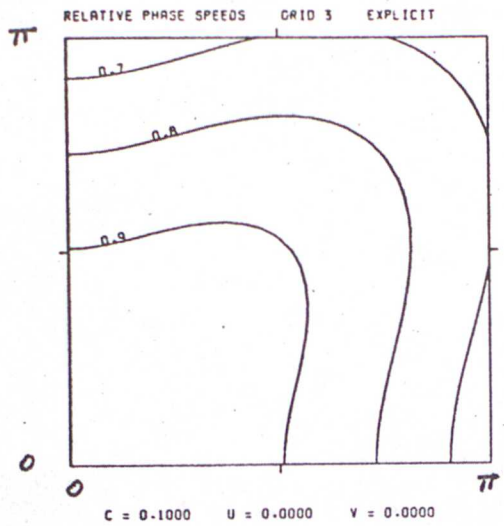

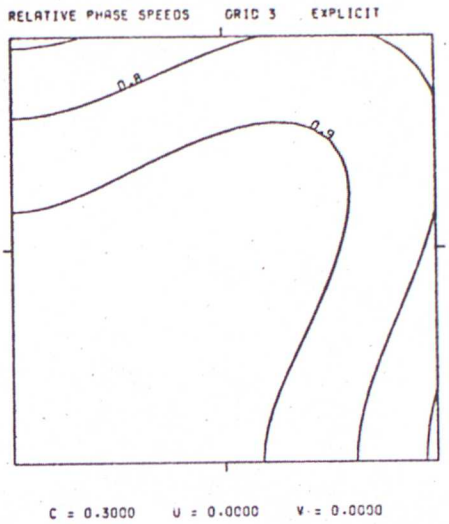

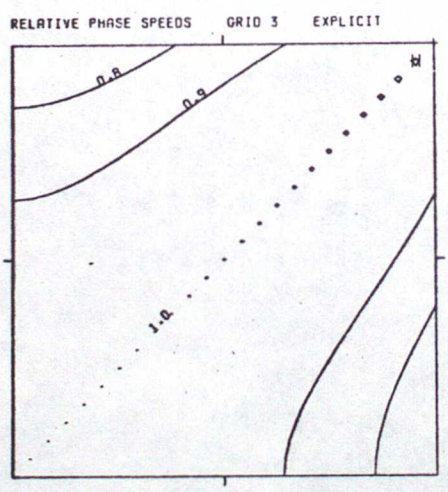

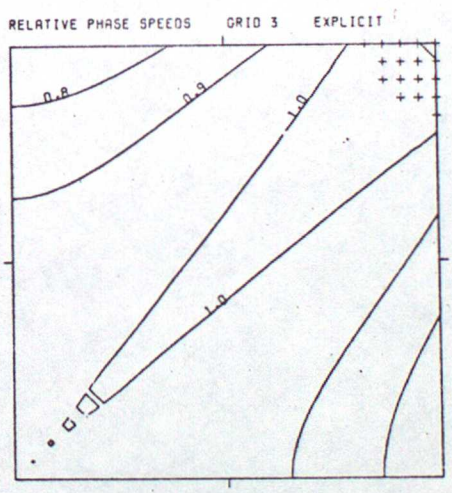

Graph 3(a) GROUP 3 EXPLICIT GRAVITY WAVES

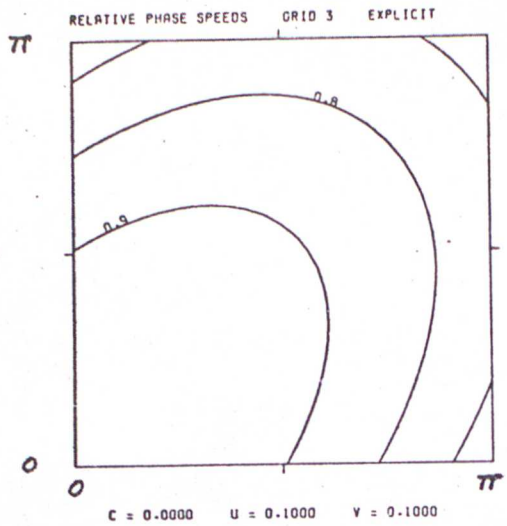

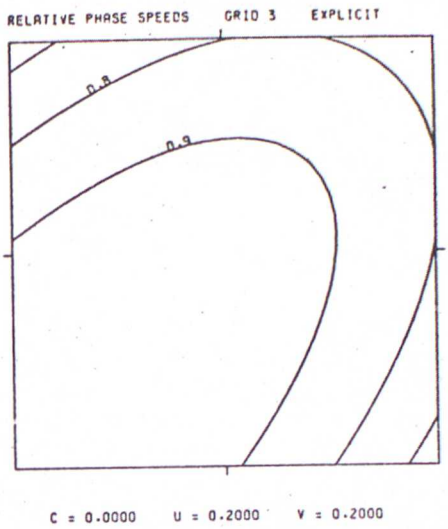

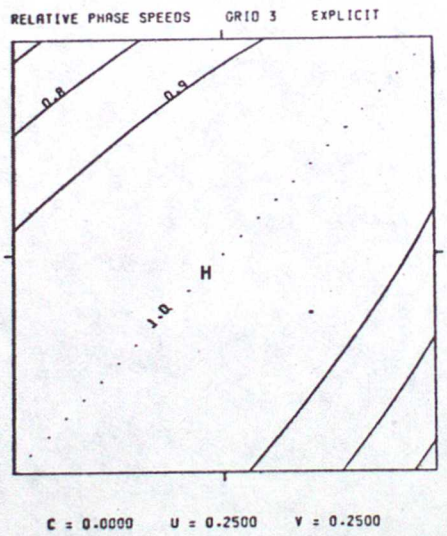

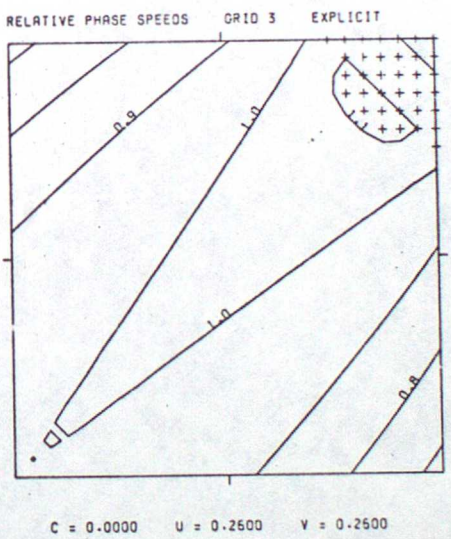

Graph 3(b) GROUP 3 EXPLICIT ADVECTION

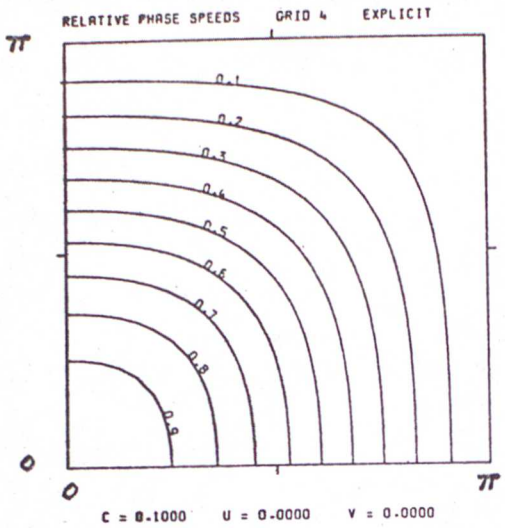

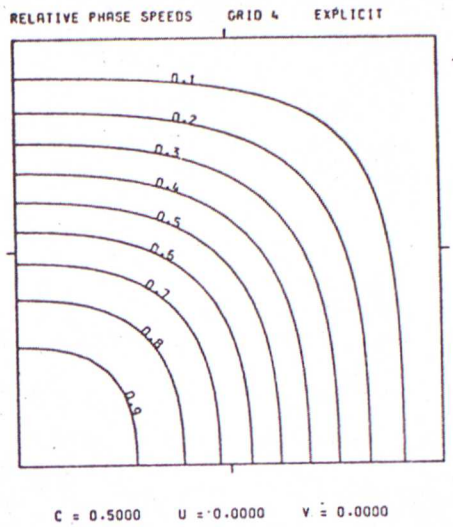

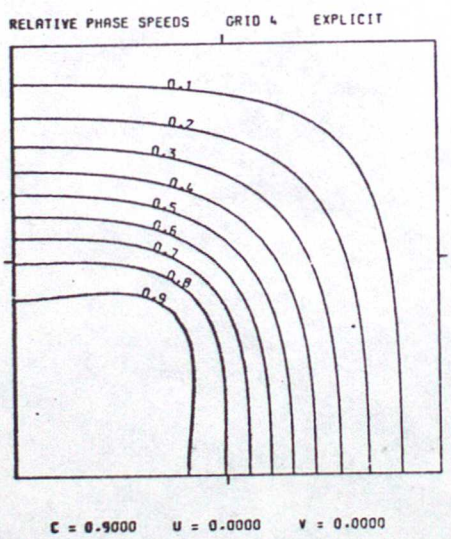

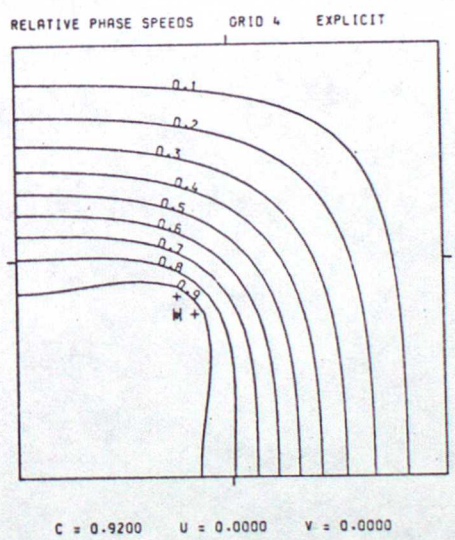

Graph 4 (a) GROUP 4 EXPLICIT GRAVITY WAVES

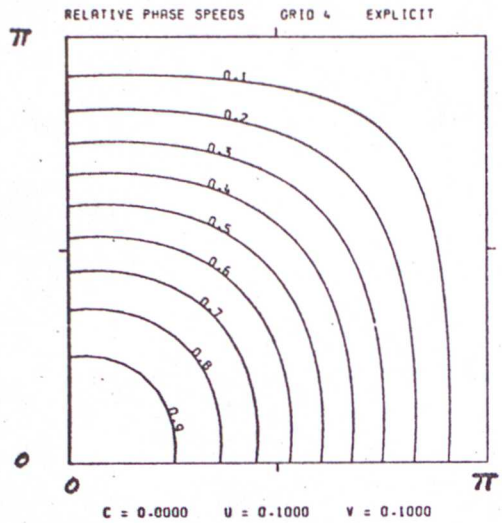

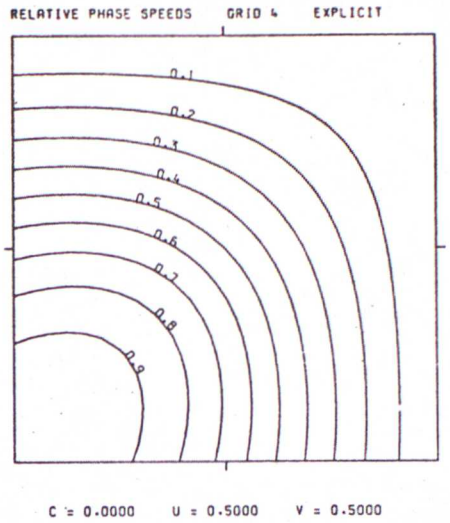

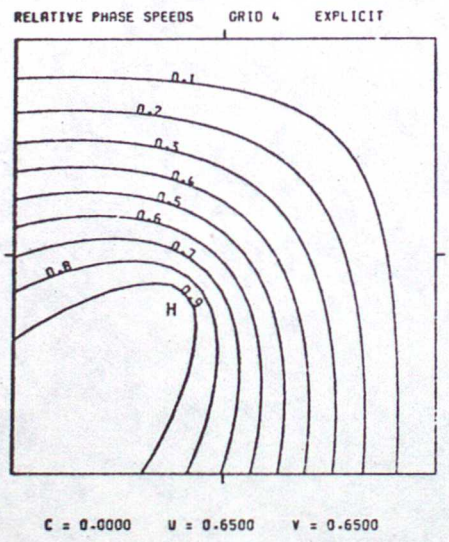

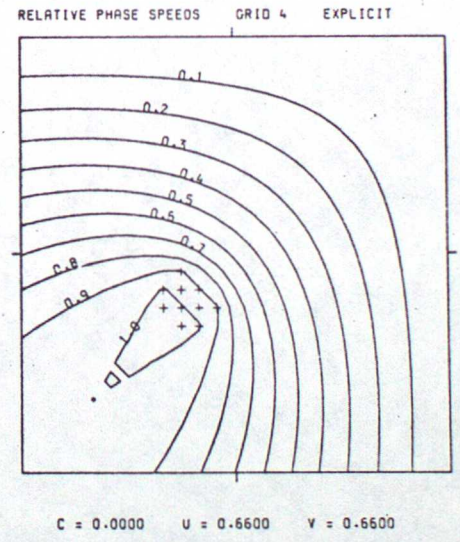

Graph 4 (b) GROUP 4 EXPLICIT ADVECTION

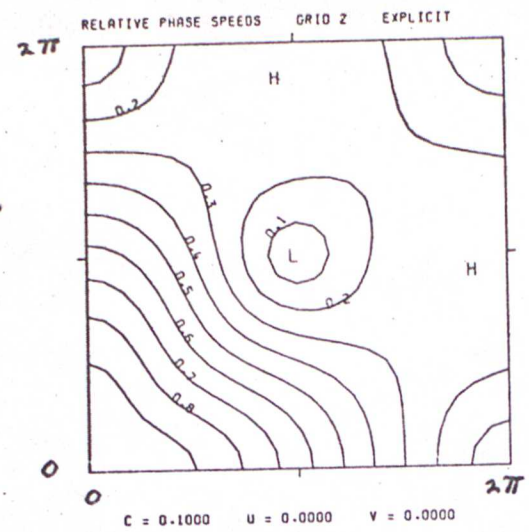

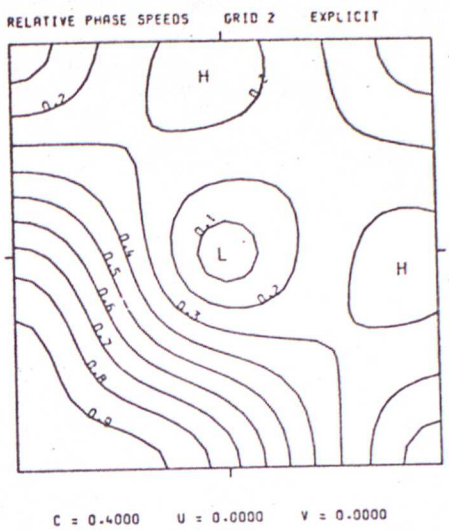

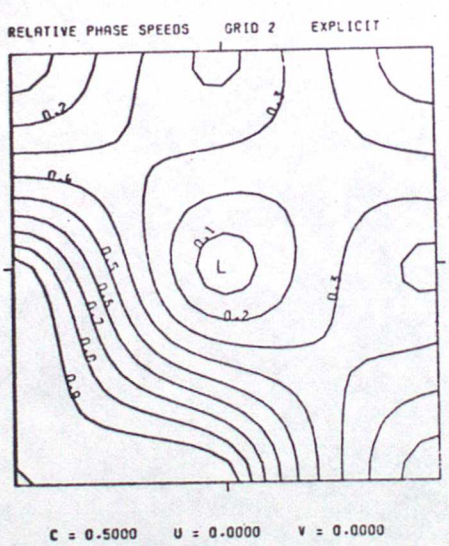

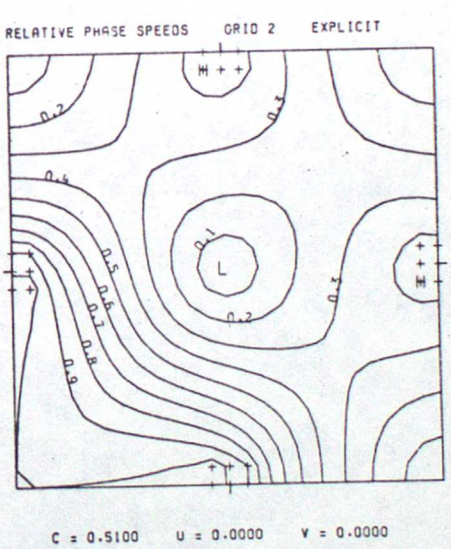

Graph 5(a) GROUP 2 EXPLICIT GRAVITY WAVES

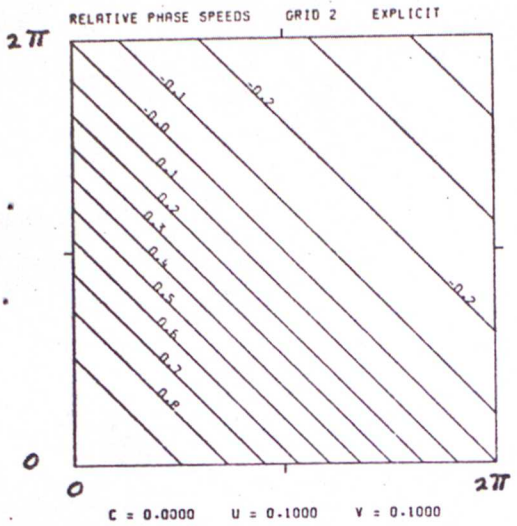

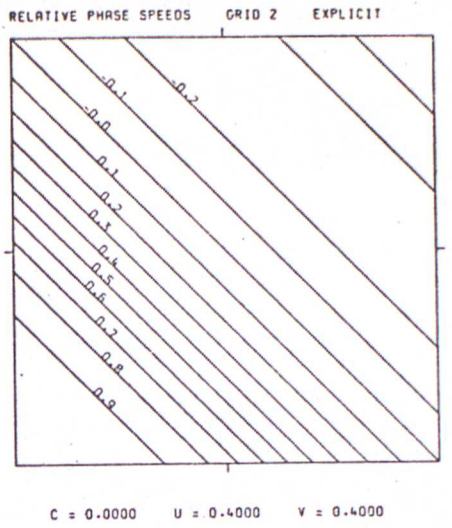

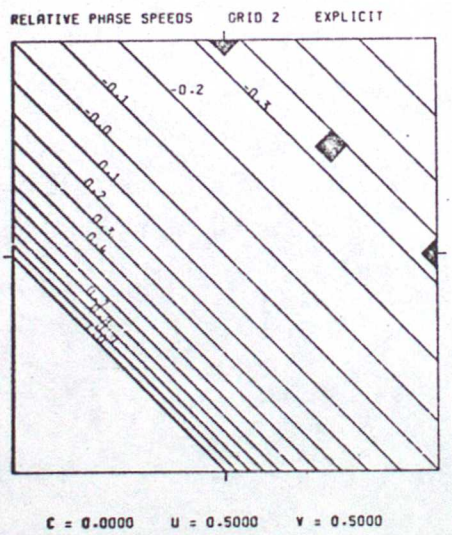

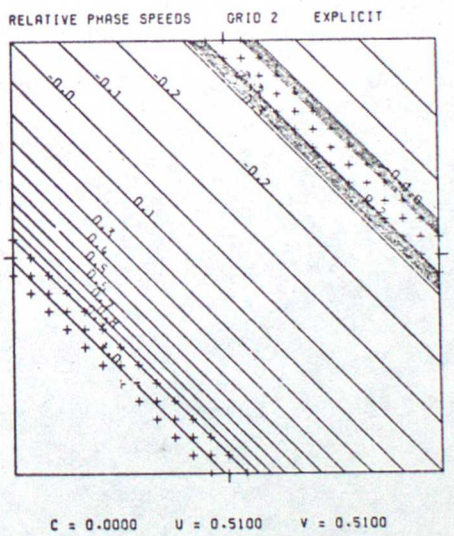

Graph 5(b) GROUP 2 EXPLICIT ADVECTION

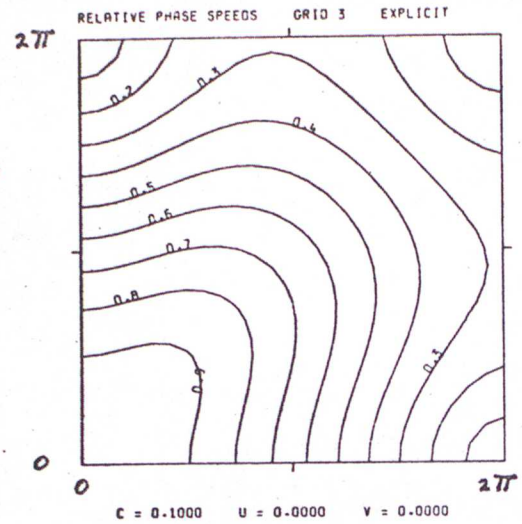

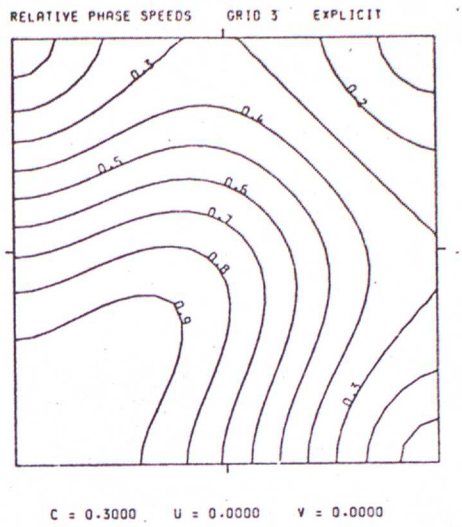

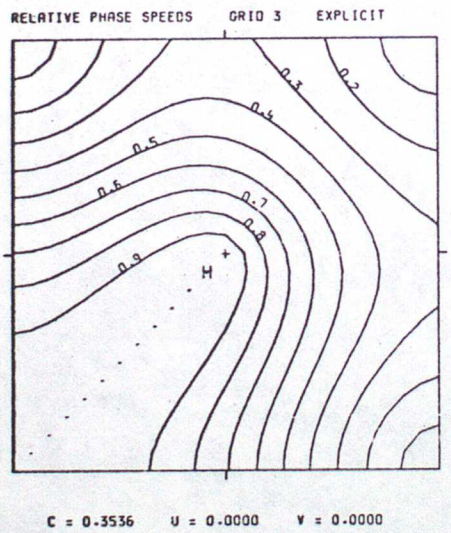

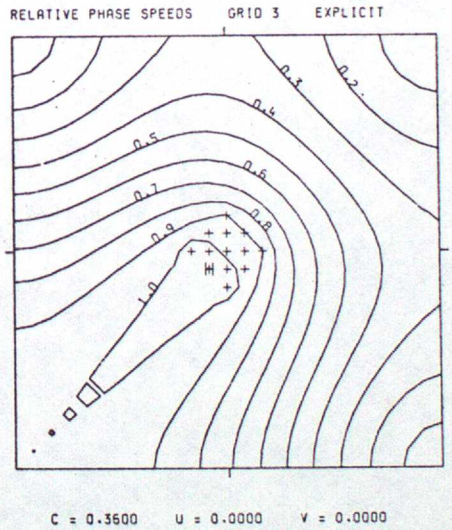

Graph 6 (a) GROUP 3 EXPLICIT GRAVITY WAVES

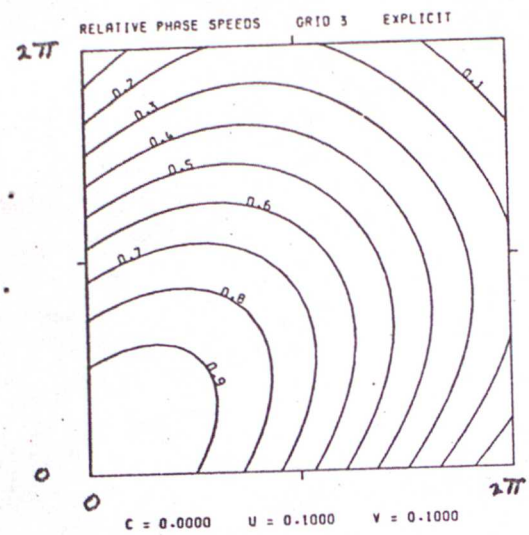

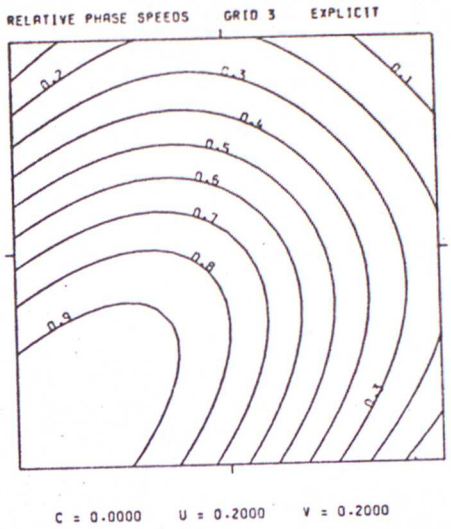

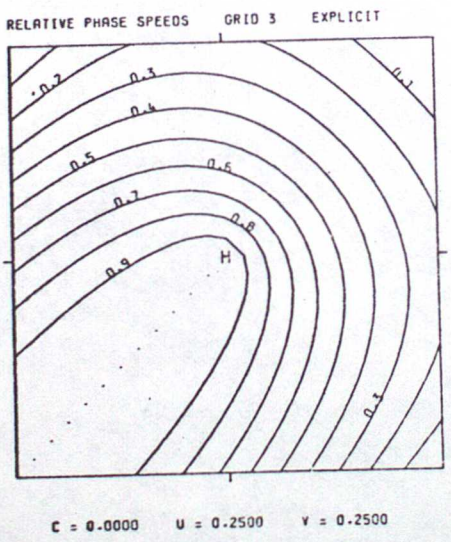

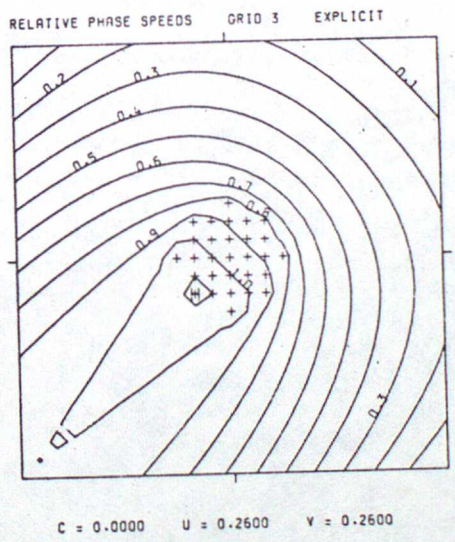

Graph 6 (b) GROUP 3 EXPLICIT ADVECTION

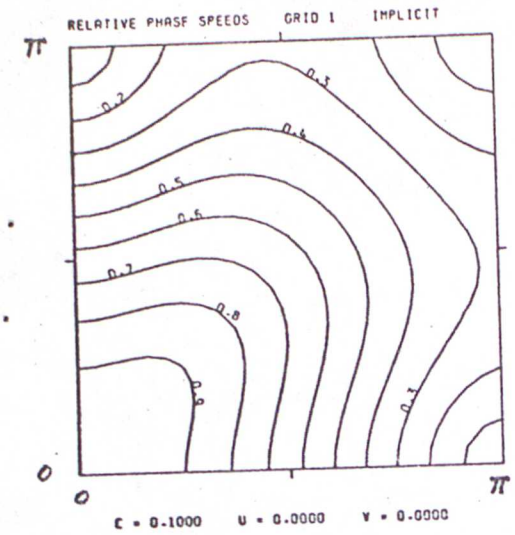

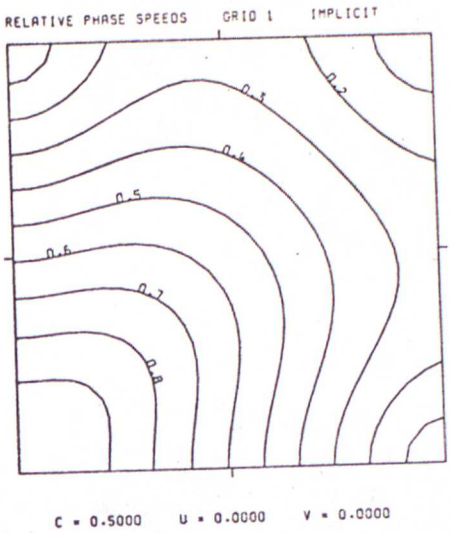

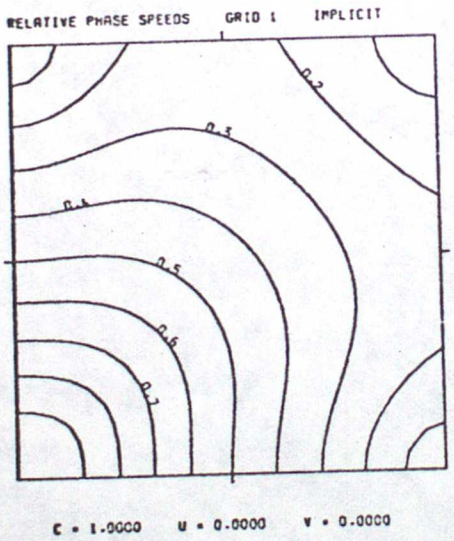

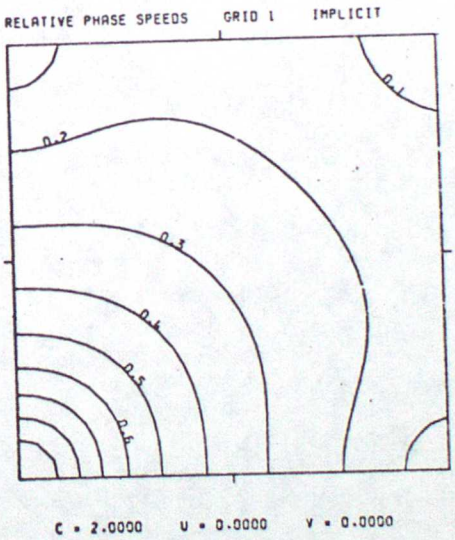

Graph 7 (a) GROUP 1 IMPLICIT GRAVITY WAVES

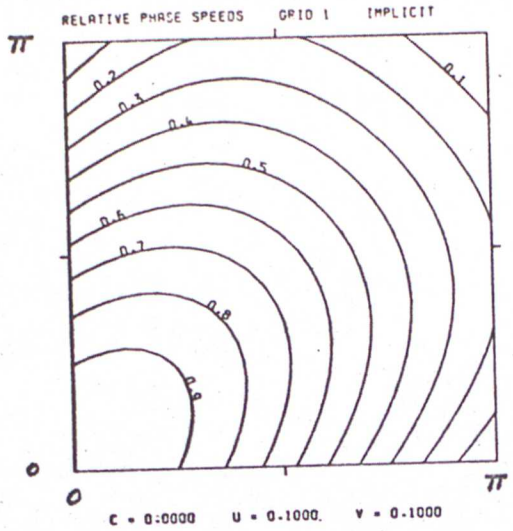

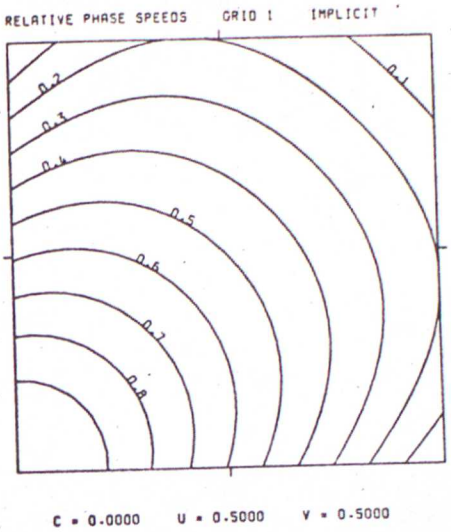

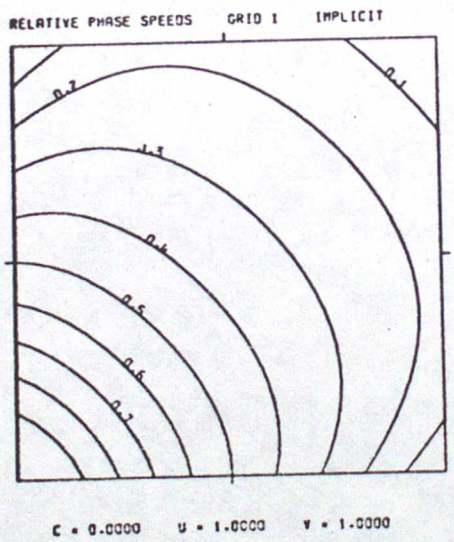

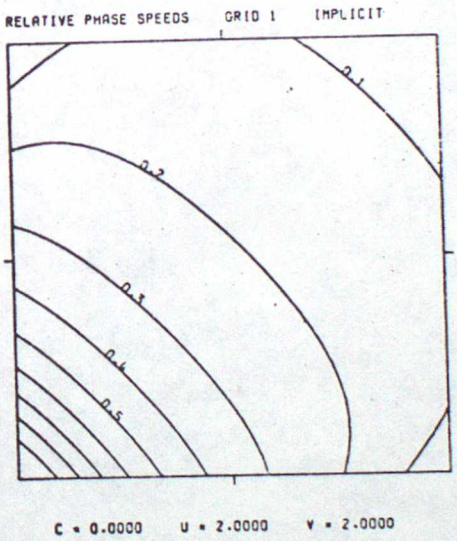

Graph 7 (b) GROUP 1 IMPLICIT ADVECTION

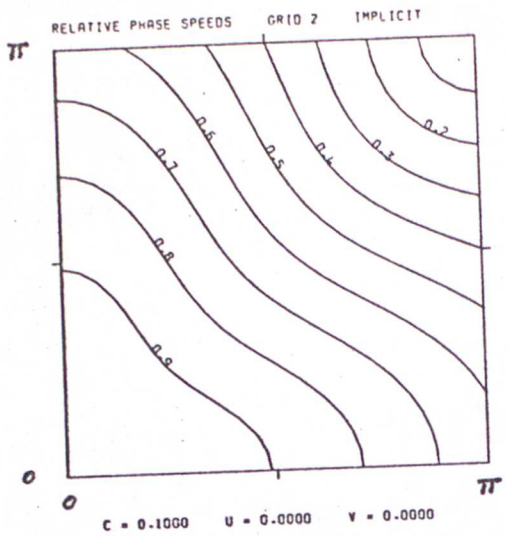

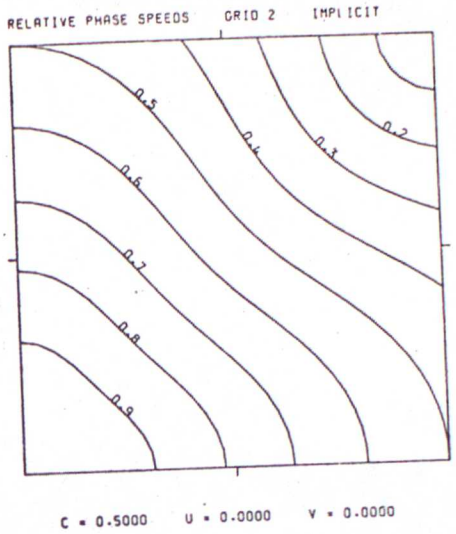

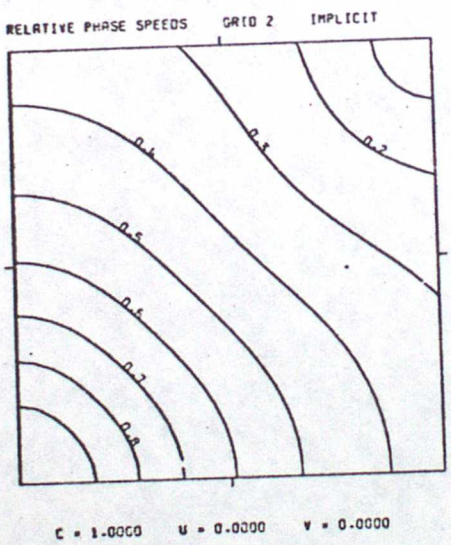

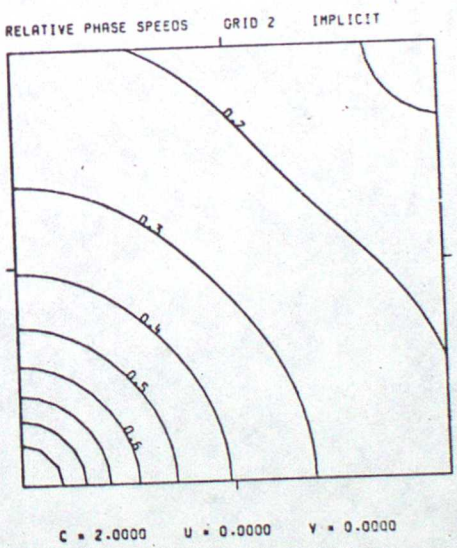

Graph 8 (a) · GROUP 2 IMPLICIT GRAVITY WAVES

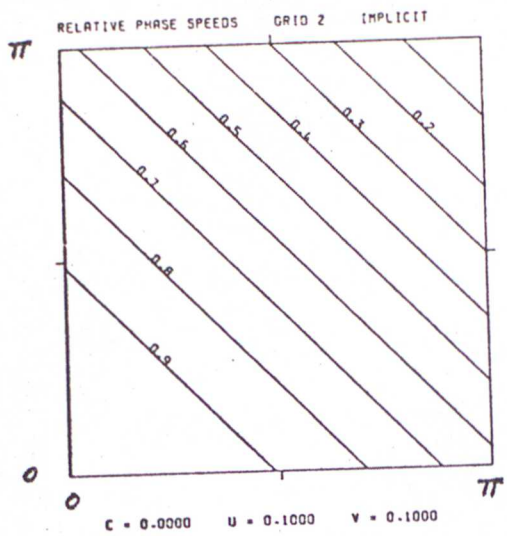

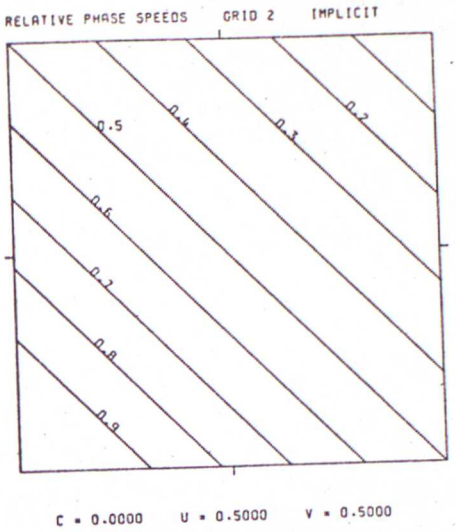

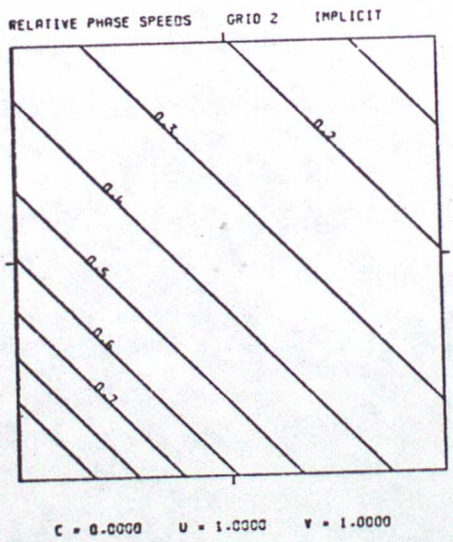

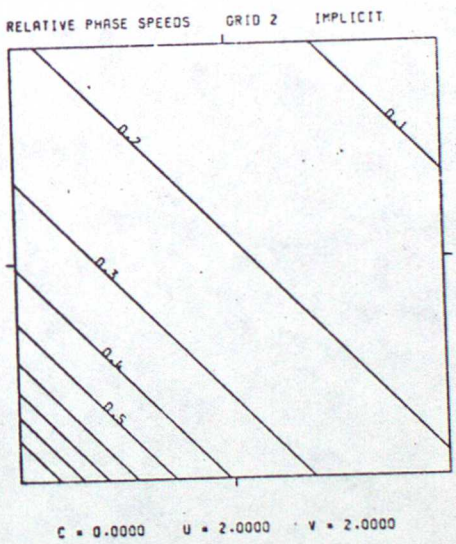

Graph 8 (b) GROUP 2 IMPLICIT ADVECTION

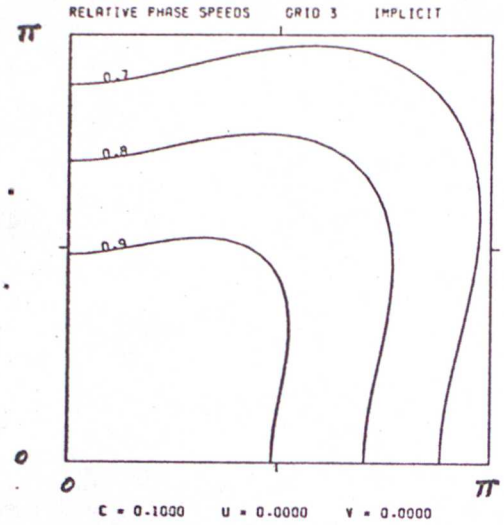

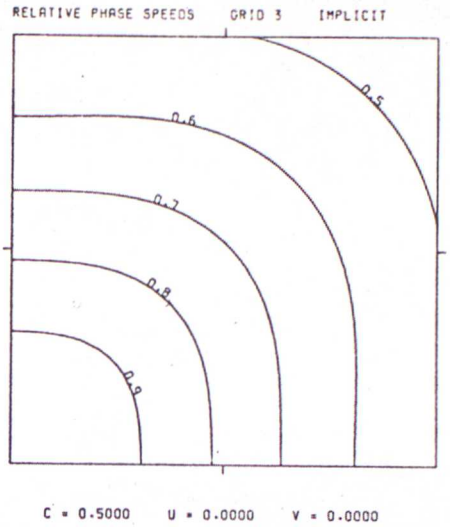

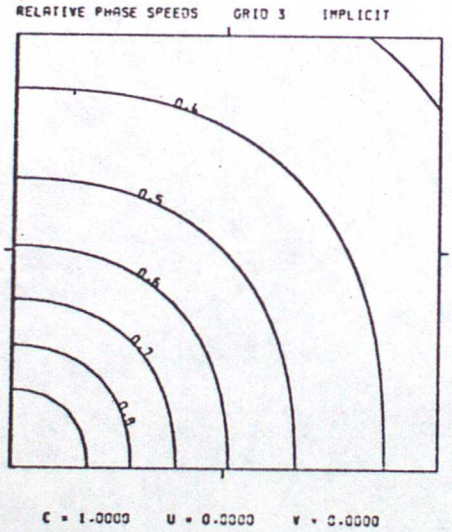

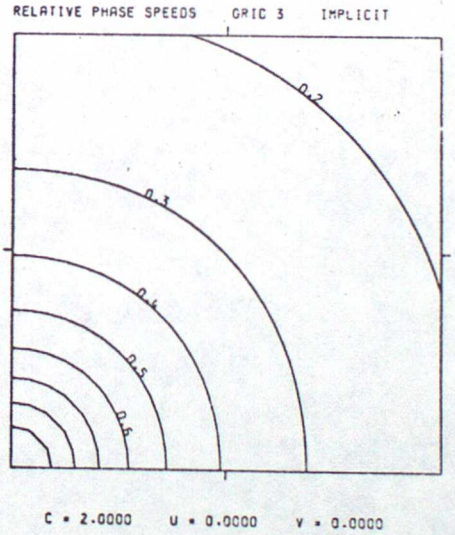

Graph 9 (a) GROUP 3 IMPLICIT GRAVITY WAVES

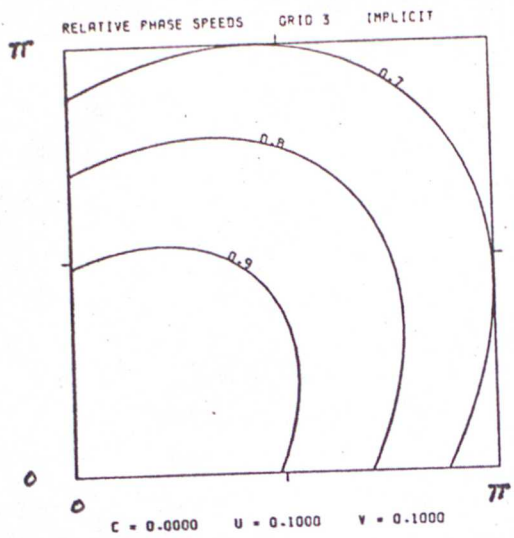

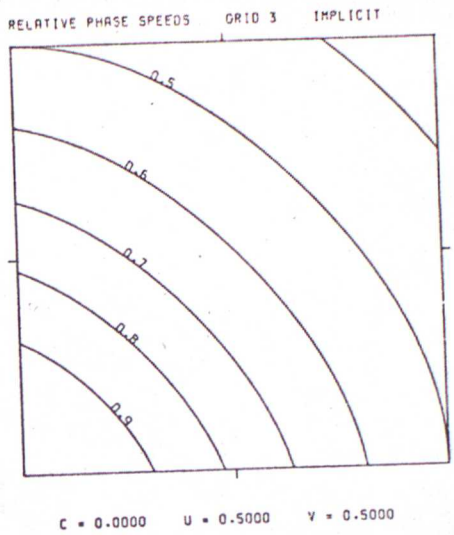

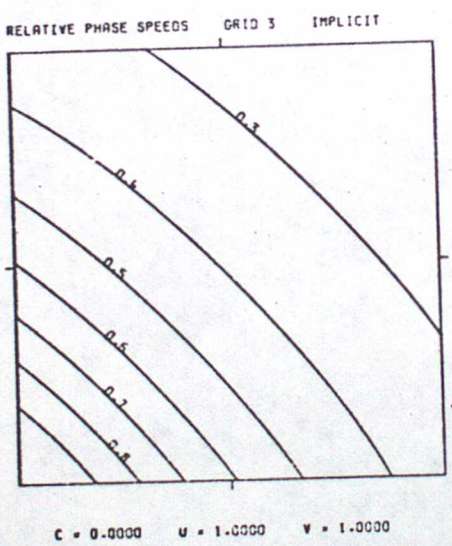

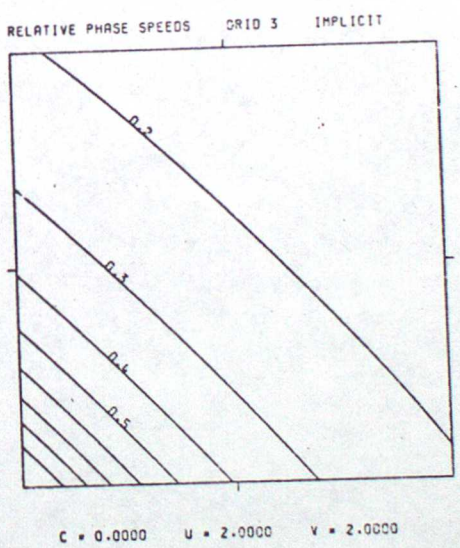

Graph 9 (b) GROUP 3 IMPLICIT ADVECTION

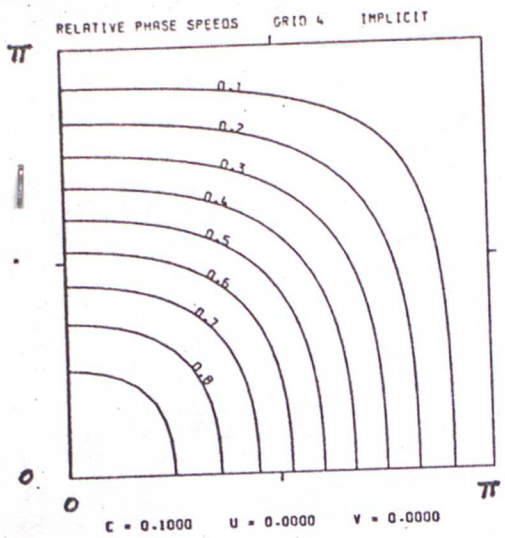

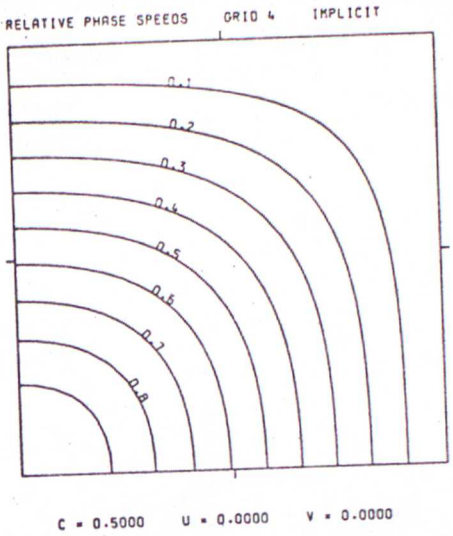

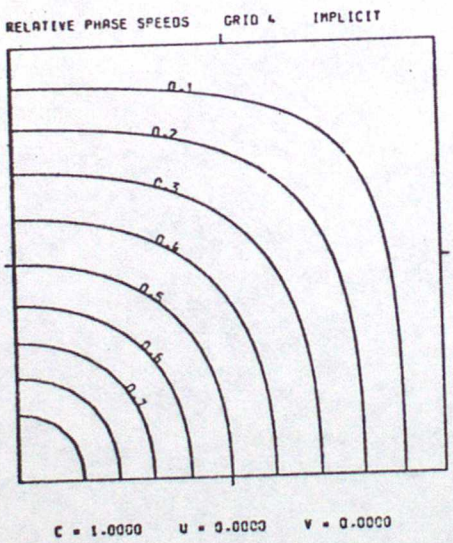

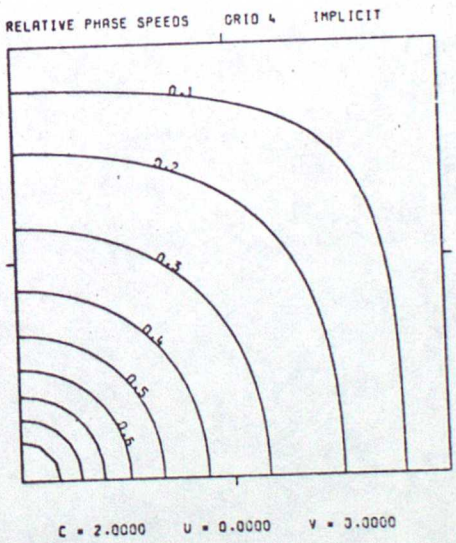

Graph 10(a) GROUP 4 IMPLICIT GRAVITY WAVES

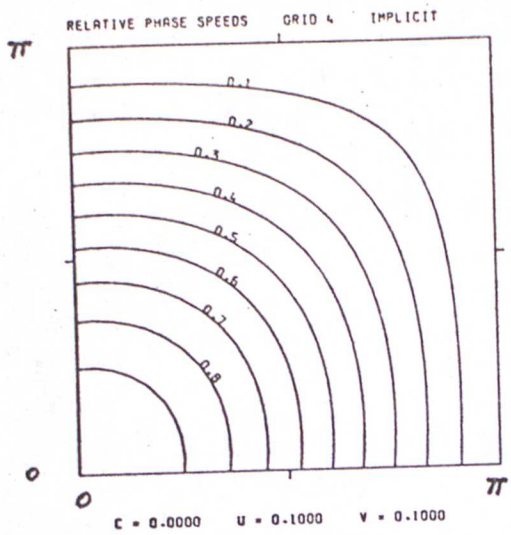

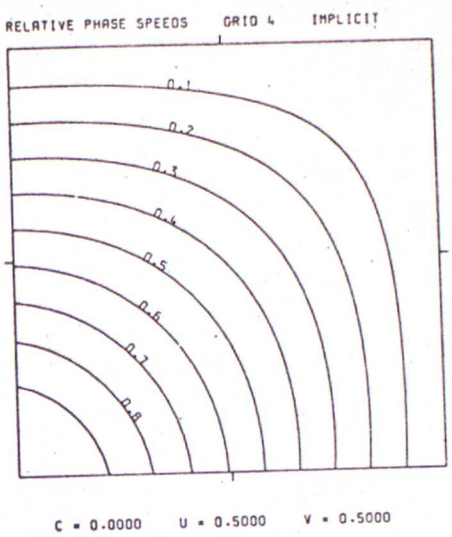

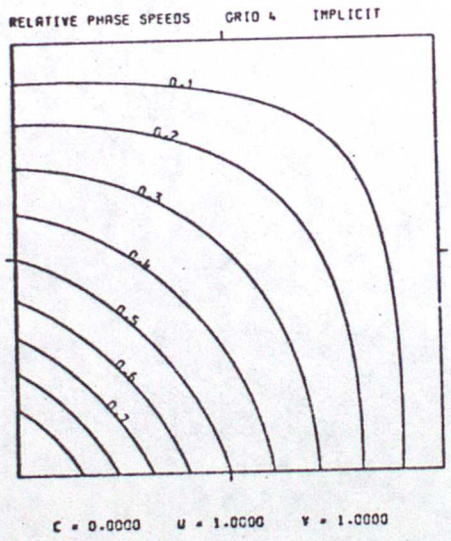

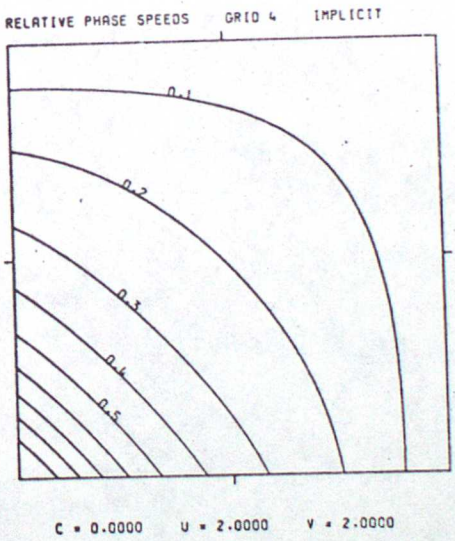

Graph 10(b) GROUP 4 IMPLICIT ADVECTION

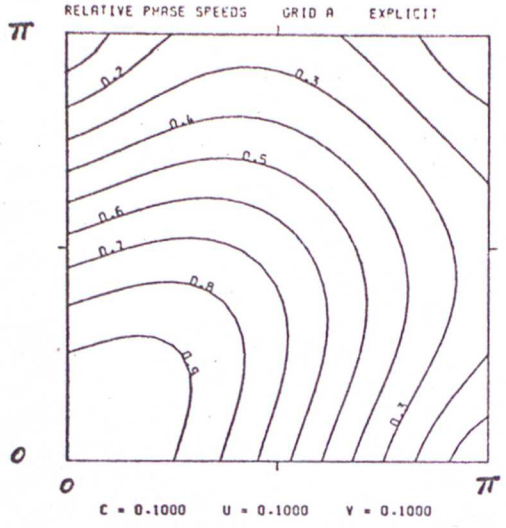

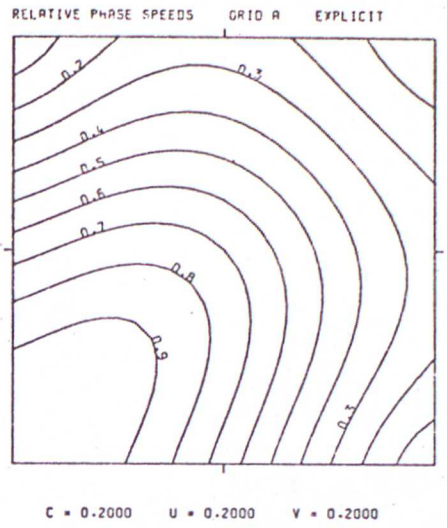

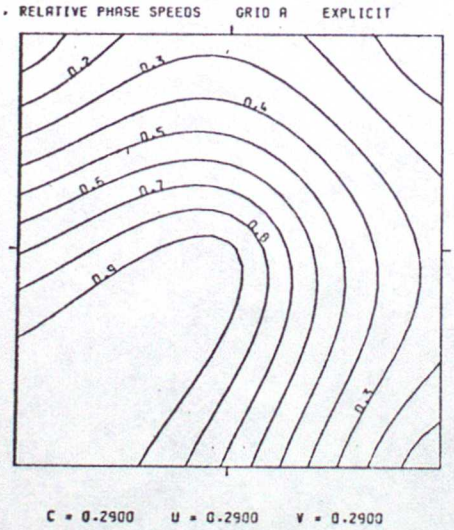

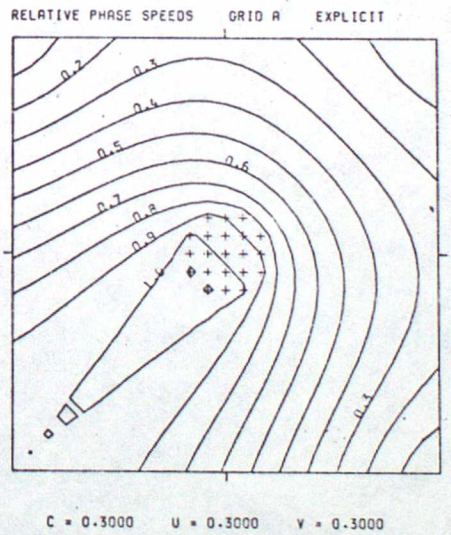

Graph 11 GRID A EXPLICIT SHALLOW WATER WAVES

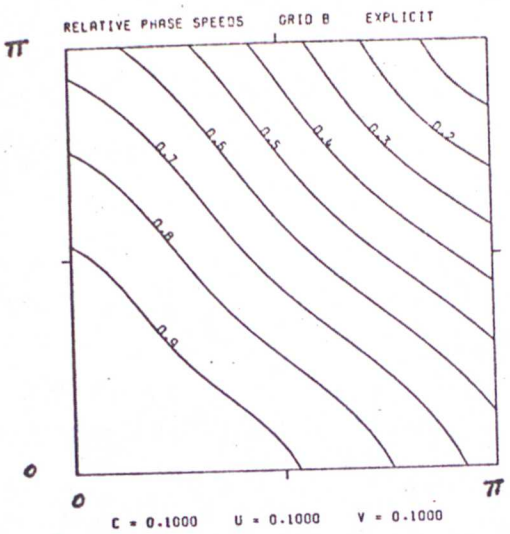

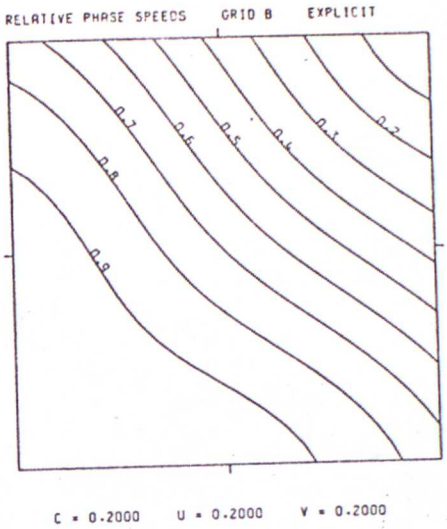

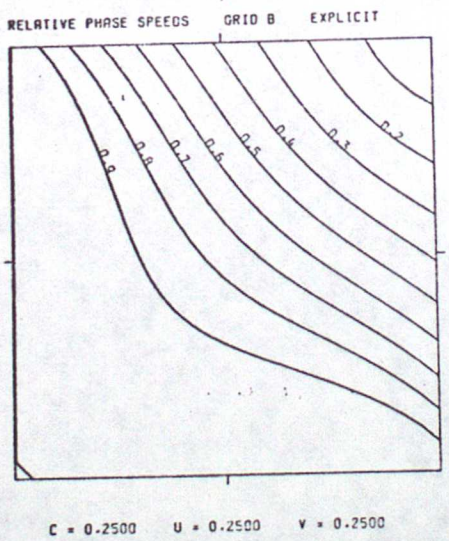

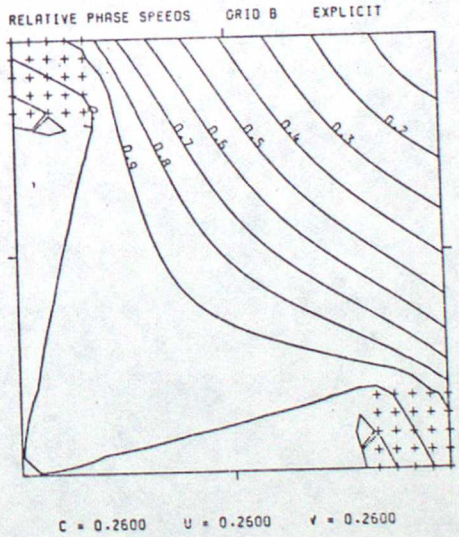

Graph 12 GRID B EXPLICIT SHALLOW WATER WAVES

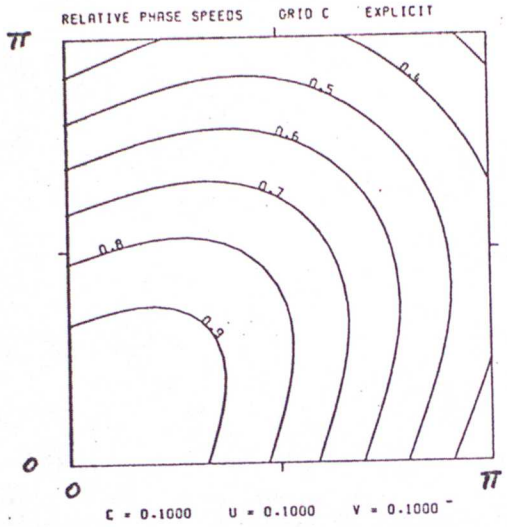

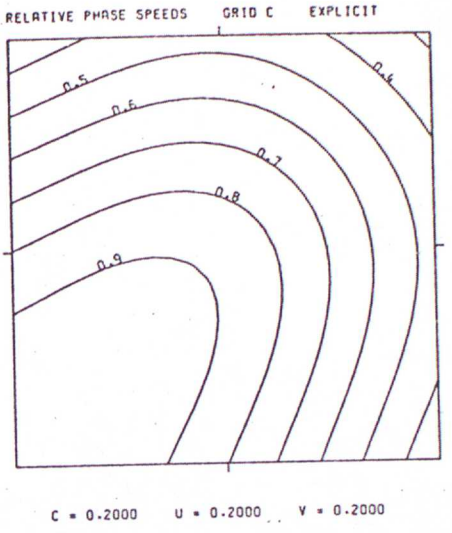

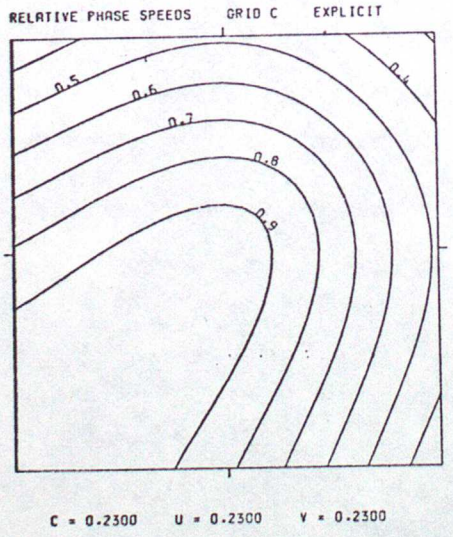

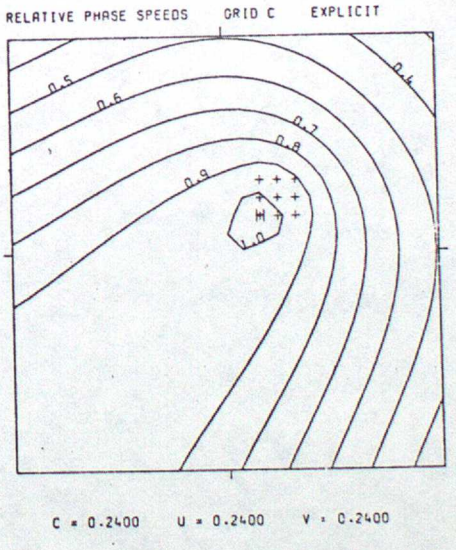

Graph 13 GRID C EXPLICIT SHALLOW WATER WAVES

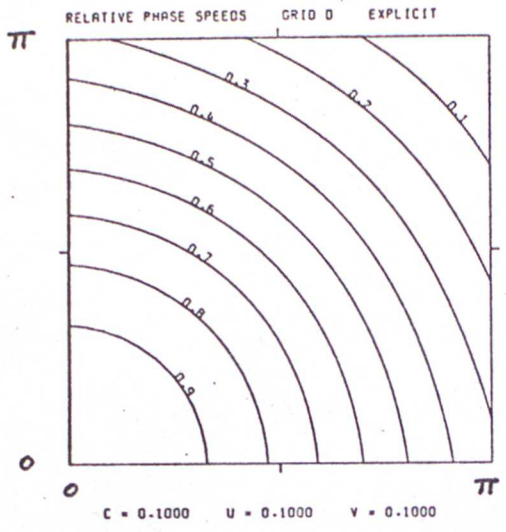

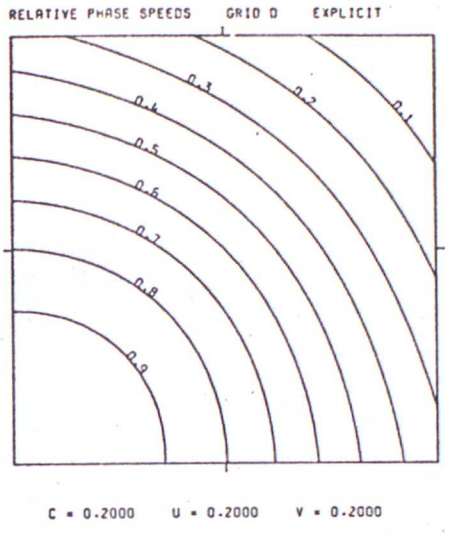

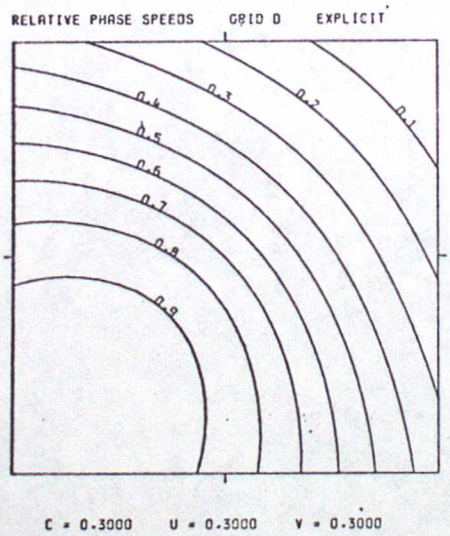

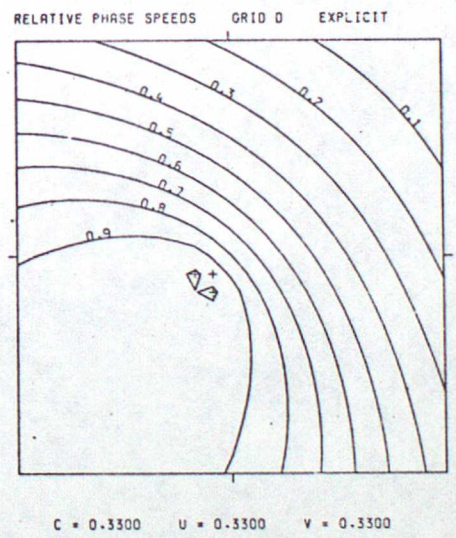

Graph 14 GRID D EXPLICIT SHALLOW WATER WAVES

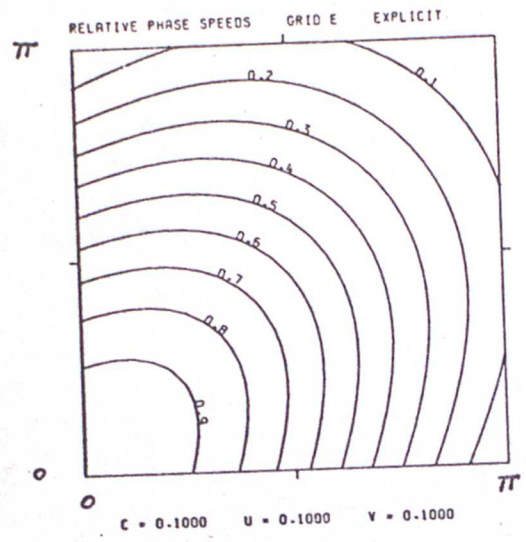

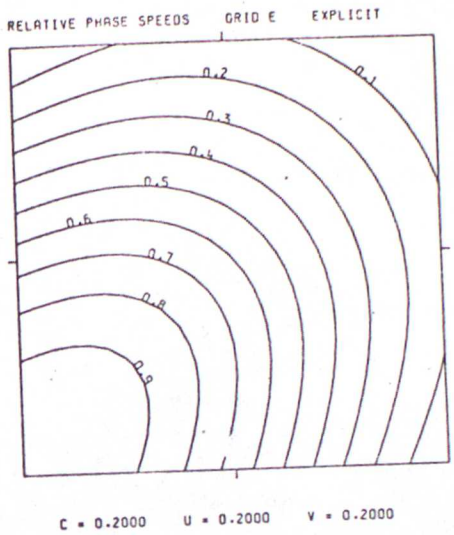

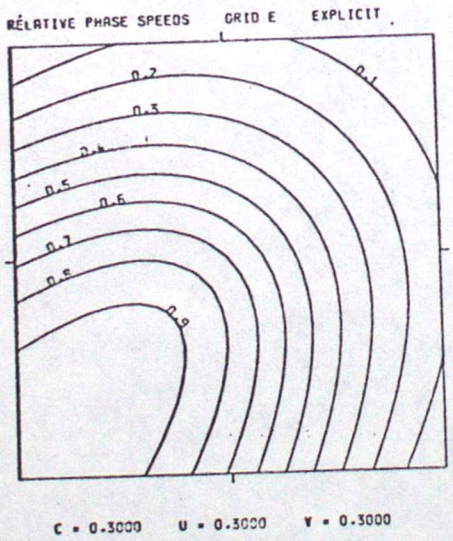

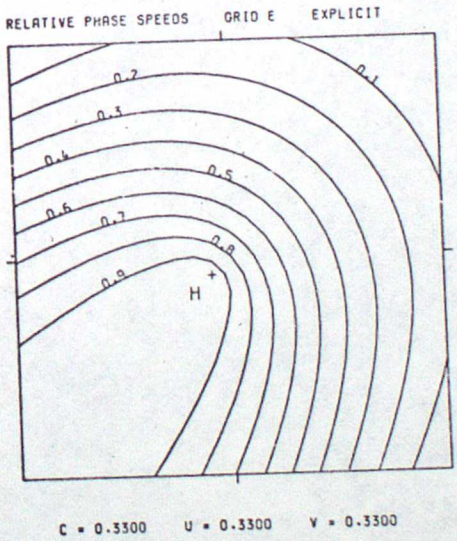

Graph 15 GRID E EXPLICIT SHALLOW WATER WAVES

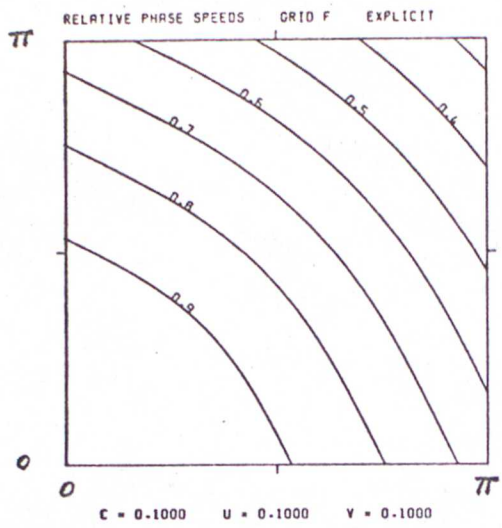

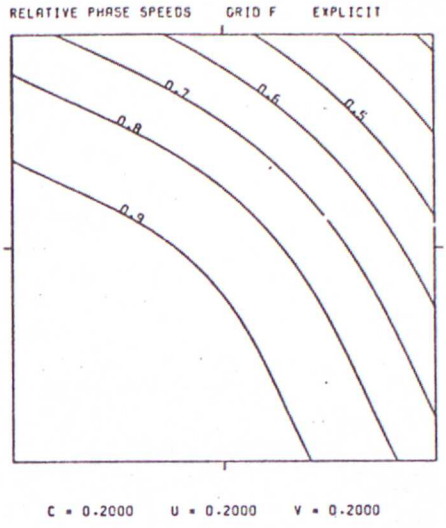

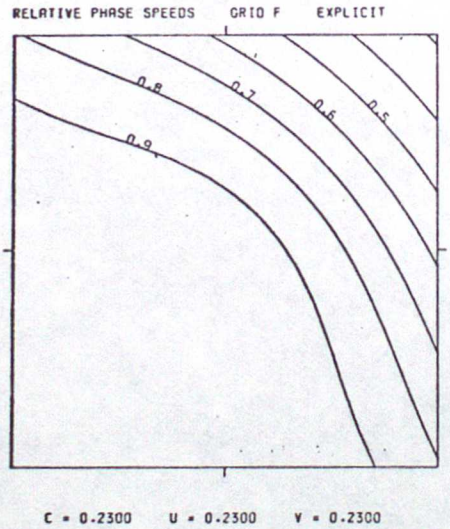

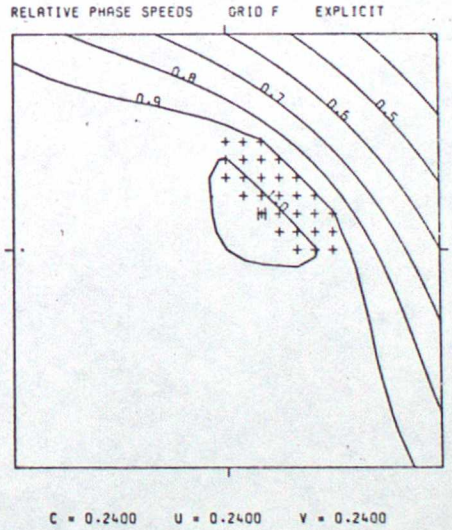

Graph 16 GRID F EXPLICIT SHALLOW WATER WAVES

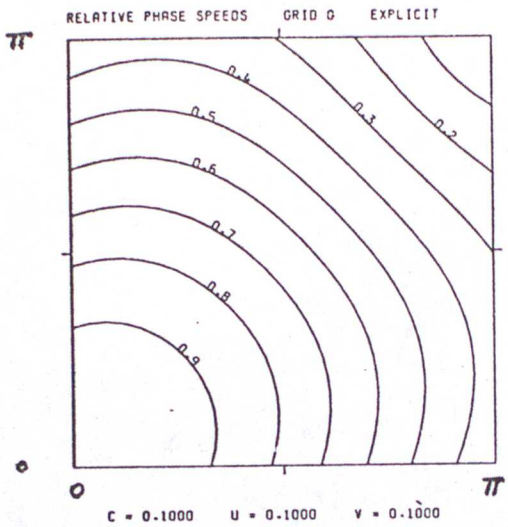

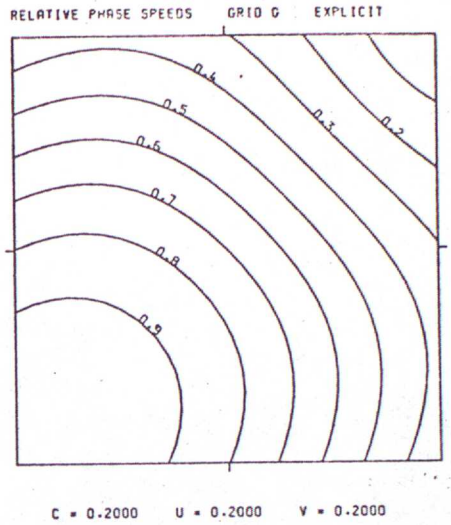

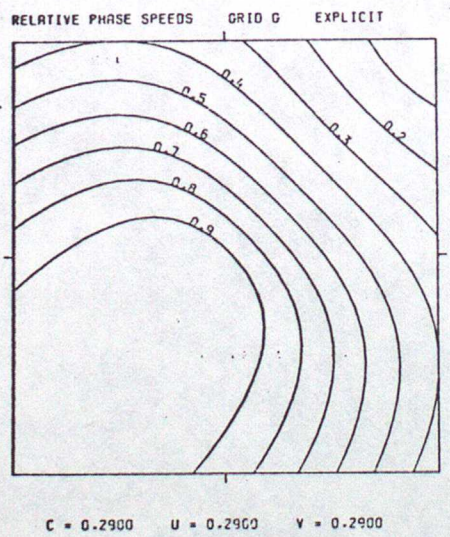

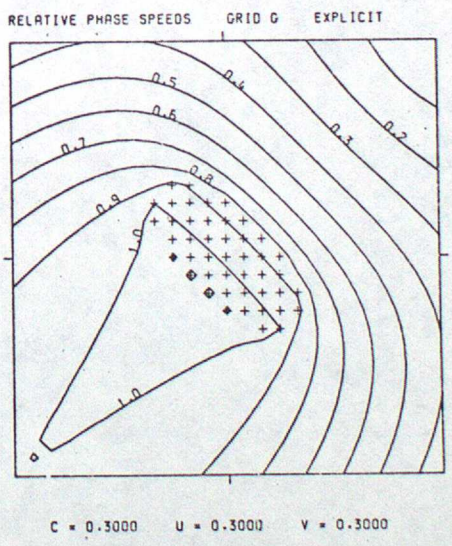

Graph 17 GRID G EXPLICIT SHALLOW WATER WAVES

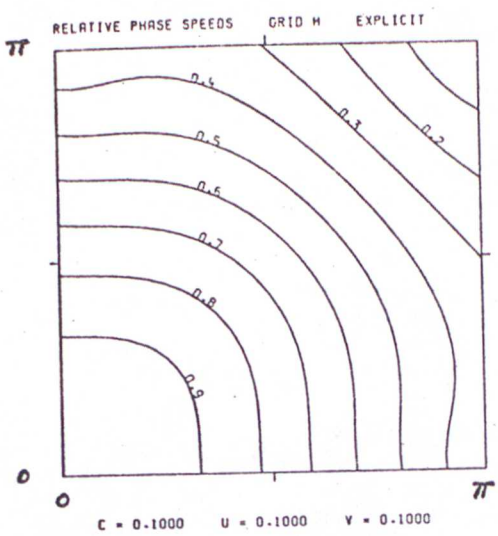

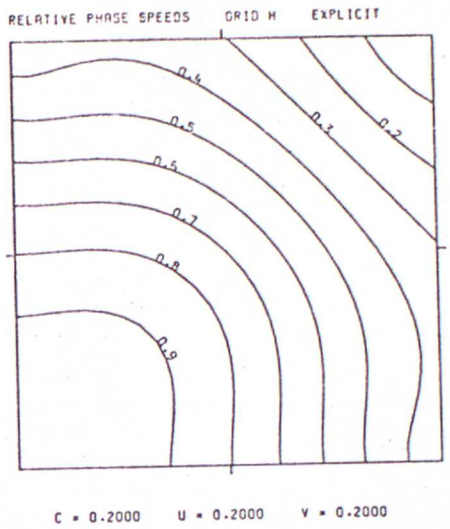

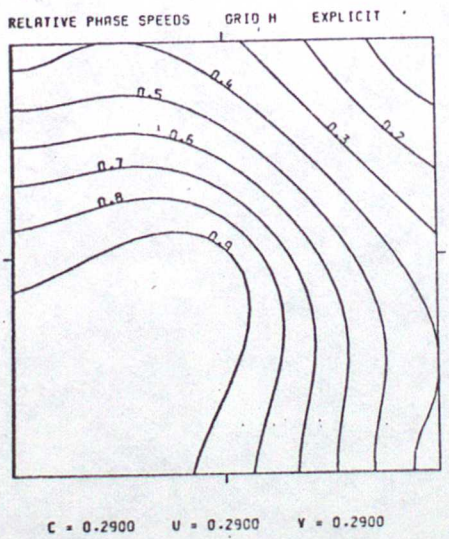

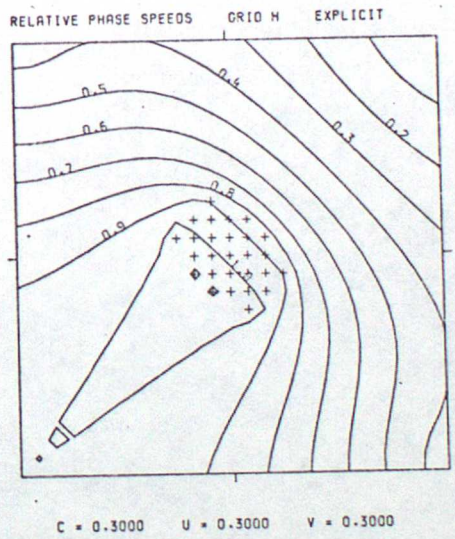

Graph 18 GRID H EXPLICIT SHALLOW WATER WAVES

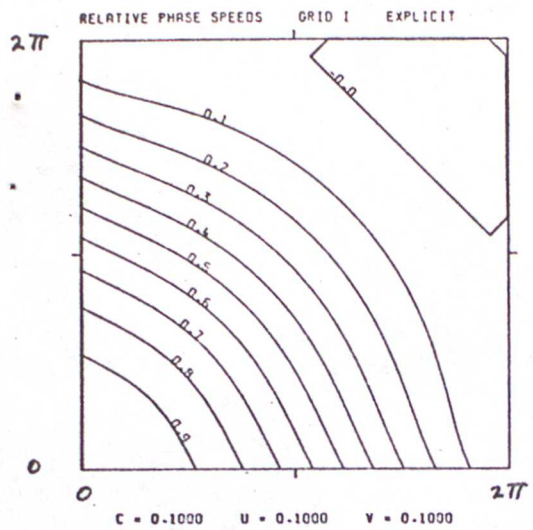

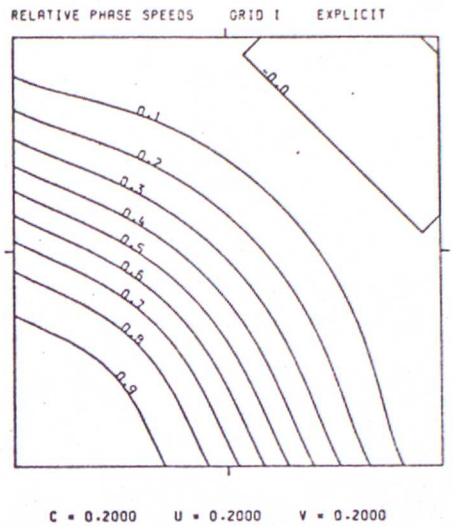

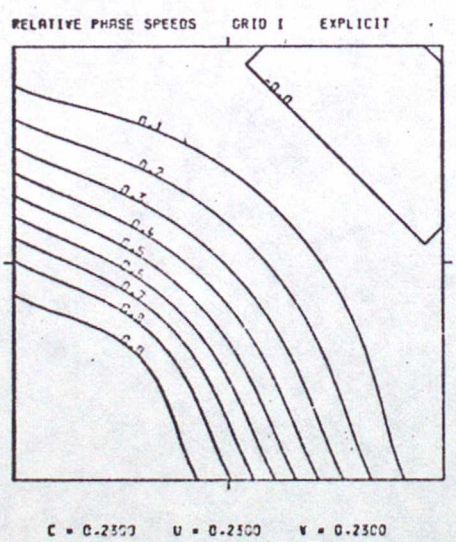

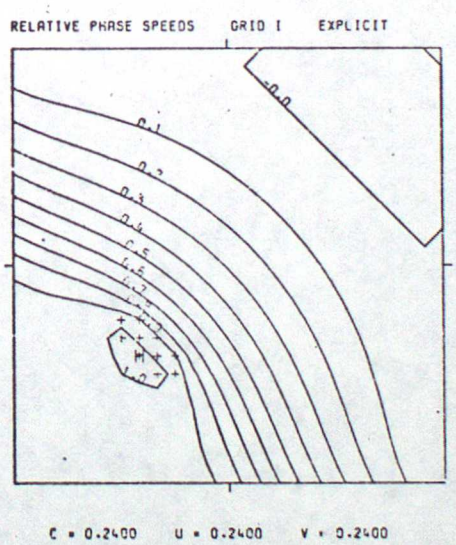

Graph 19 GRID I EXPLICIT SHALLOW WATER WAVES

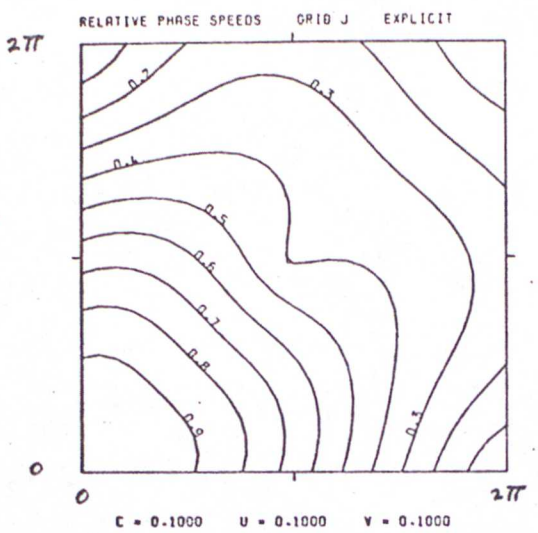

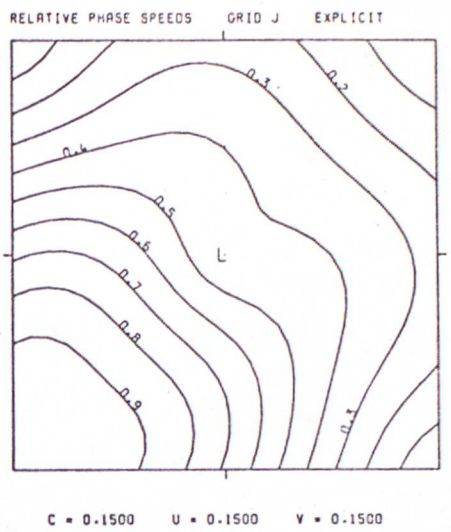

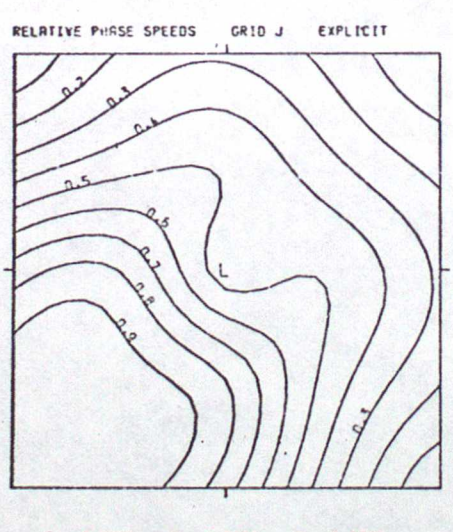

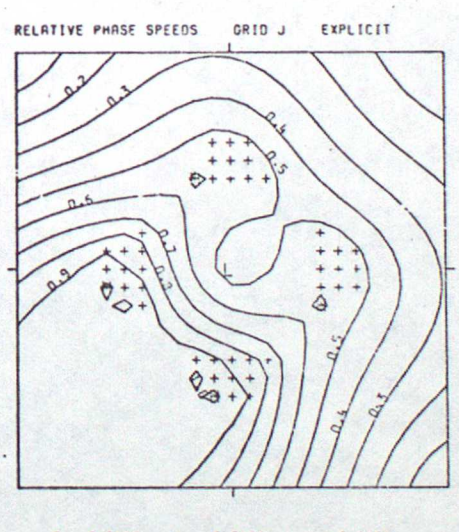

Graph 20 GRID J EXPLICIT SHALLOW WATER WAVES

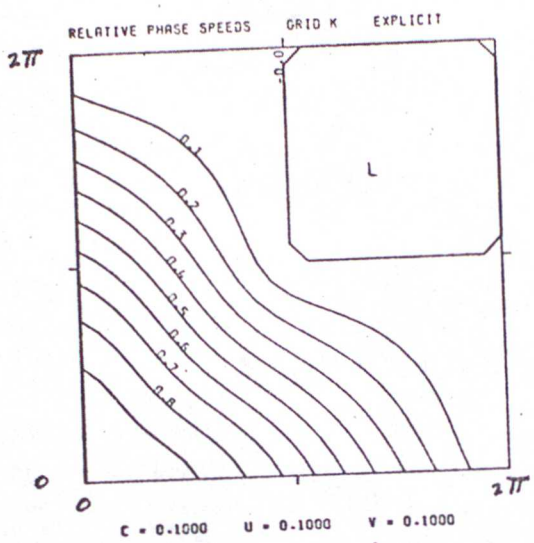

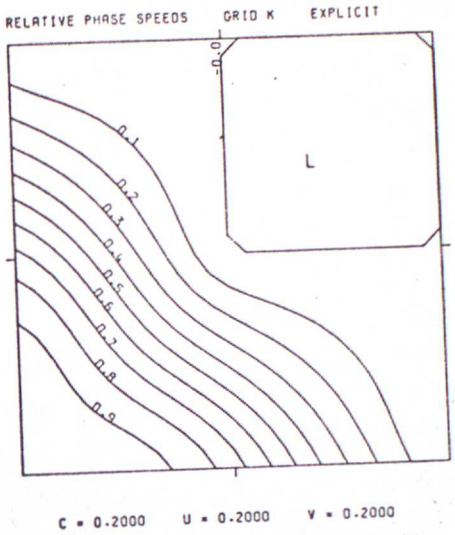

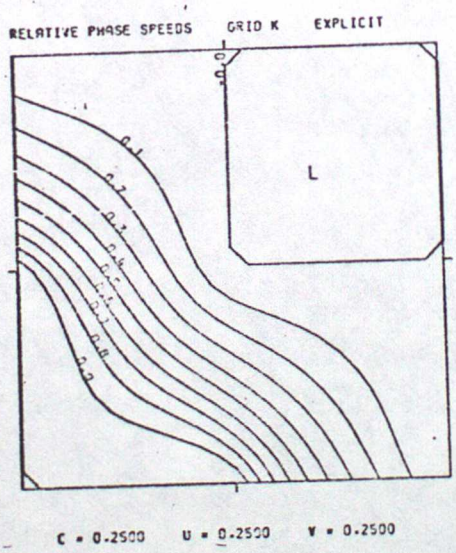

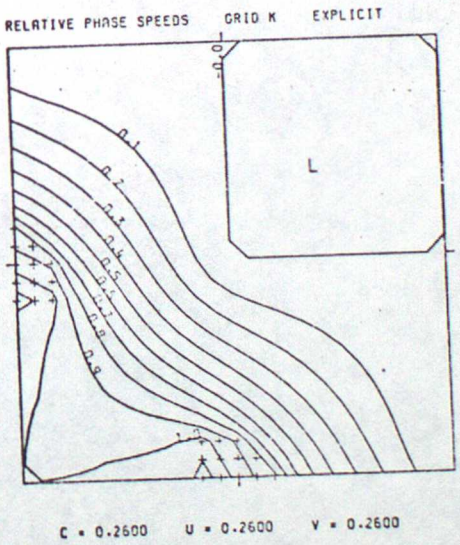

Graph 21 GRID K EXPLICIT SHALLOW WATER WAVES

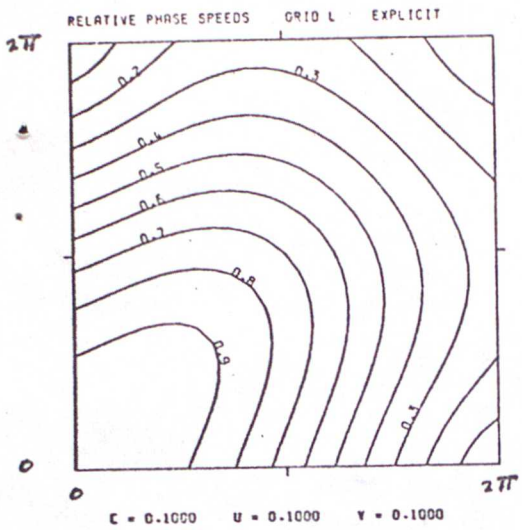

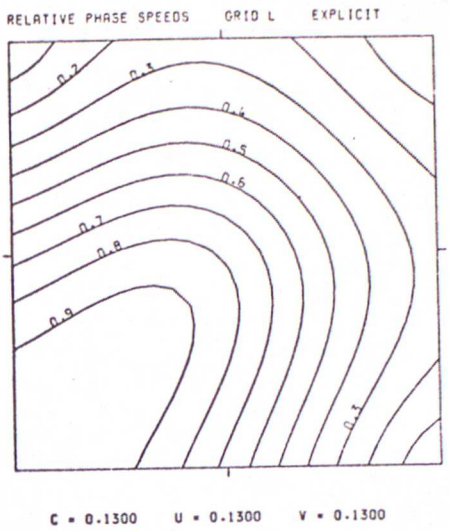

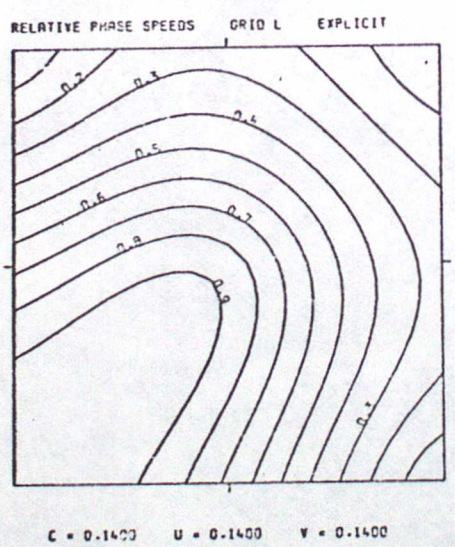

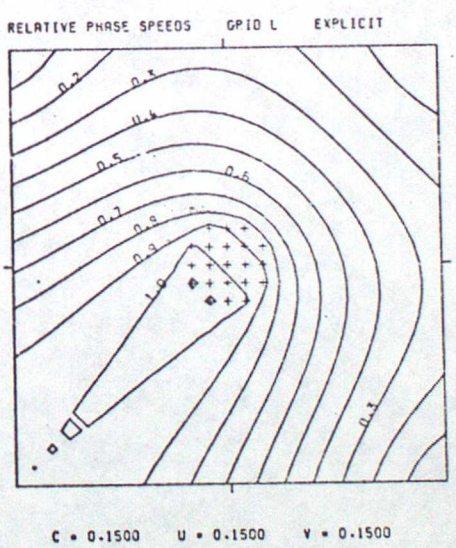

Graph 22 GRID L EXPLICIT SHALLOW WATER WAVES